Hyperuniformity at the Absorbing State Transition: Perturbative RG for Random Organization

Xiao Ma[1], Johannes Pausch[1,2] Gunnar Pruessner[2] and Michael E. Cates[1]

1 DAMTP, Centre for Mathematical Sciences, University of Cambridge, Wilberforce Road, Cambridge CB3 0WA, United Kingdom
2 Department of Mathematics, Imperial College, London SW7 2AZ, United Kingdom

Abstract

Hyperuniformity, in which the static structure factor or density correlator obeys $S(q) \sim q^\varsigma$ with $\varsigma > 0$, emerges at criticality in systems having multiple, symmetry-unrelated, absorbing states. Important examples arise in periodically sheared suspensions and amorphous solids; these lie in the random organisation (RO) universality class. Here, using Doi-Peliti field theory for interacting particles and perturbative RG about a Gaussian model, we find $\varsigma = 0^+$ and $\varsigma = 2\epsilon/9 + O(\epsilon^2)$ in dimension $d > d_c = 4$ and $d = 4 - \epsilon$ respectively. Our calculations assume that renormalizability is sustained via a certain pattern of cancellation of strongly divergent terms. These cancellations allow the upper critical dimension to remain $d_c = 4$, as is known to hold for RO, whereas generic perturbations (*e.g.*, those violating particle conservation) would typically flow to a fixed point with $d_c = 6$. The assumed cancellation pattern is closely reminiscent of a long-established one near the tricritical Ising fixed point. (This has $d_c = 3$, although generic perturbations flow instead towards the Wilson-Fisher fixed point with $d_c = 4$.) We show how hyperuniformity in RO emerges from anticorrelation of strongly fluctuating active and passive densities. Our one-loop calculations also yield the remaining RO exponents to order ϵ, surprisingly without recourse to functional RG methods. These exponents coincide as expected with the Conserved Directed Percolation (C-DP) class which also contains the Manna Model and the quenched Edwards-Wilkinson (q-EW) model. Importantly however, our ς exponent differs from one found via a mapping to q-EW. In that mapping, ς is calculated by discarding an irrelevant conserved noise term. Here we argue that this term is *dangerously* irrelevant, allowing ς to change value. Thus, although other exponents are common to both, the RO and C-DP universality classes have different exponents for hyperuniformity.

Contents

1   Introduction

Any configuration that a system can enter, but not escape from, is called an absorbing (or inactive) state. A continuous 'absorbing-state transition' arises when the probability of surviving indefinitely, for a system in the thermodynamic limit of infinite size, falls continuously to zero upon varying a control parameter such as particle density [1, 2].

Of particular interest are cases where there are many distinct absorbing states that are unrelated by symmetry. For example, experiments on non-Brownian particles of number density ρ supended in a fluid, subject to slow periodic shearing of fixed amplitude, show that at large ρ particles collide and are randomly displaced each cycle: there is always a finite density, ρ_A, of 'active' particles. In contrast, below a critical density, $\rho = \rho_c$, particles 'randomly organize'

into a non-colliding, stroboscopically static, disordered state in which all particles are passive: $\rho \equiv \rho_A + \rho_P = \rho_P$ [3–5]. At the critical density, this state of random organization (RO) takes infinitely long to appear, and acquires infinitely long-range correlations as is generic at a second order phase transition. Approaching from within the active phase ($\rho \to \rho_c^+$), the correlation length and time diverge continuously with universal critical exponents [1–6].

Remarkably, the emergent spatial correlations are 'hyperuniform', a term meaning that long-range density fluctuations are completely supressed [7]. Thus in RO, avoidance of collisions requires emergence of a highly correlated configuration in which density fluctuations *vanish* at low wavenumbers q, rather than *diverge* as in equilibrium criticality. In dimensions $d = 2, 3$, the static structure factor at criticality vanishes as a power law: $\langle \rho_{\mathbf{q}} \rho_{-\mathbf{q}} \rangle \equiv \delta^d(0) S(q) \sim q^\varsigma$ with $\varsigma > 0$ [8,9]. Scaling arguments then give $S(0) \sim \xi^{-\varsigma}$ at large but finite correlation length ξ. These phenomena are not limited to sheared colloids, but are generic for systems in which a nonconserved, diffusive scalar order parameter (ρ_A), is coupled locally to a conserved density (ρ), such that there are multiple absorbing states ($\rho_A = 0$) of different frozen density patterns $\rho_P(x)$. This scenario defines the Random Organisation, or RO, universality class.

Until now, the RO class has been assumed identical to a larger one that also includes several different-looking models, including the Manna model of sandpiles [10–12], conserved directed percolation (C-DP) [1, 2], and the quenched Edwards-Wilkinson model (q-EW) of interfacial growth. The q-EW correspondence uses a mapping [13–15] in which the interfacial height is the time-integrated active particle density, $u(t) = \int_0^t \rho_A(s) ds$, while the random field evaluated at height u gives ρ_P. (Both freeze at the depinning transition.) Functional renormalisation group (FRG) methods applied to q-EW [16] have allowed calculation to order ϵ^3 ($\epsilon = 4 - d$) of the C-DP exponents, with the one-loop results being $\beta = 1 - \epsilon/9$, $\nu_\perp = \frac{1}{2} + \epsilon/12$ and $z = 2 - 2\epsilon/9$ [14, 15], describing the vanishing of the order parameter ($\rho_A \sim (\rho - \rho_c)^\beta$), and the divergences of the correlation length ($\xi \sim (\rho - \rho_c)^{-\nu_\perp}$) and time ($\mathcal{T} \sim \xi^z$). Since the passive particle density field ρ_P is mapped to the random quenched field and integrated out of the q-EW action, it becomes difficult to interpret either the total density field ρ or hyperuniformity. Nevertheless, arguing that the evolution of the total density field is subject to the deterministic diffusion of active particles only and not to any relevant dynamical noise, an exact mapping between ρ and ρ_A yields the hyperuniformity exponent $\varsigma = 0 + \epsilon/3$ [17]. (This calculation of [17] was in part motivated by a pre-publication version of the present work [18].)

In this paper, we find ς to order ϵ for RO by instead using a perturbative RG (not FRG) for a Doi-Peliti field theory of interacting particles [19–21]. Our hyperuniformity exponent, $\varsigma = 0 + 2\epsilon/9$, differs from the one obtained via the q-EW mapping in [17]. This discrepancy is not a contradiction, but linked to the emergence of two distinct physical scenarios corresponding to the presence (our result) or absence (q-EW result) of *diffusive conservative noise* in the dynamics of the active particles [6, 15, 22]. The two different calculations of ς can both be correct if the conservative noise is *dangerously irrelevant*, and therefore capable of changing the exponents for correlation functions while leaving the remaining exponents intact [23]. In effect, the diffusive noise splits the RO/C-DP/q-EW universality class into two sub-classes for the purposes of studying hyperuniformity. We shall give compelling arguments that exactly this scenario does arise in RO.

Our calculations have several novel technical features which go beyond those normally encountered in perturbative RG calculations using Doi-Peliti field theories. Indeed, prior to the current work, those obstacles have prevented a perturbative field-theoretic calculation not just of ς but of the standard RO/C-DP/q-EW exponents ($\beta, \nu_\perp, z$). Below we accomplish the calculations to one loop, subject to a set of clearly stated assumptions that are needed to resolve various ambiguities that arise.

As well as finding ς, we recover to order ϵ the known values of $\beta, \nu_\perp, z$. This offers a pow-

erful check on our assumptions: it would be a remarkable coincidence for all three exponents to emerge from a perturbative theory that was not well-founded. One may wonder how we can find these results perturbatively, when others have argued that FRG is required to deal with an infinite number of relevant operators [16]. Yet, because the FRG is performed on the opposite side of the C-DP/q-EW mapping, which involves a non-trivial infinite summation of individual Doi-Peliti operators, this is not necessarily a contradiction.

En route to our perturbative RG results, we examine our interacting particle theory at Gaussian level, applicable for $d > d_c = 4$. (Even this requires a careful treatment of tree-level diagrams.) Surprisingly, we also find a type of hyperuniformity here, albeit of a singular form that can be viewed as an exponent of $\varsigma = 0^+$. This resolves uncertainty [24, 25] over whether hyperuniformity persists in high dimensions where the Gaussian theory should hold. The Gaussian theory lays bare a significant feature of RO (hinted at in [8]): the fluctuations of ρ_A and ρ_P are not separately hyperuniform even as those of $\rho = \rho_A + \rho_P$ become so. This requires near-perfect anticorrelation between the two particle types, which our Gaussian results expose, and our RG results further illuminate. Notably again, we find that the conservative noise plays a central role in the hyperuniformity found at Gaussian level. Indeed, we will see that discarding this noise creates a conservation law on the centre of mass of the particle density distribution, which is known to have drastic effects, including the occurrence of hyperuniformity throughout the active phase rather than just at the critical point [26].

Our calculations therefore (i) unveil the true character of the RO transition, with hyperuniformity emerging from cancellation of large active and passive fluctuations; (ii) directly compute the hyperuniformity exponent as $\varsigma = 0^+$ for $d > 4$ and $\varsigma = 2\epsilon/9 + O(\epsilon^2)$ for $d < 4$, as well as recovering the known exponents to this order without recourse to FRG methods; and (iii) strongly suggest that conservative noise is required to fully understand the RO universality class whose hyperuniformity exponent is then governed by this (dangerously) irrelevant term in the action.

This paper is structured as follows. In Section 2, we start by discussing some of the technical difficulties in performing perturbative RG for the RO universality class, and enumerate the arguments and assumptions needed to steer a path through these difficulties. Sections 3 and 4 show calculations for critical exponents at Gaussian and one-loop level respectively, and Section 5 discusses several physical aspects of our results. We conclude briefly in Section 6.

2   Technical Challenges and Assumptions

Our RG analysis for RO broadly follows procedures for field-theoretic RG [19, 27]; its subtle distinction with Wilsonian RG is laid out in Appendix A. However, our approach is not completely standard but instead presents several technical challenges. Before moving on to the actual calculations in Sections 3 and 4, we discuss these challenges in Section 2.1. To resolve them, we make several assumptions. Briefly these are (i) universality of the RO model, subject to the role of the potentially dangerously irrelevant noise, (ii) perturbative renormalisability of the theory in Doi-Peliti formalism and (iii) emerging hyperuniformity (rather than divergent fluctuations) at the critical transition. Reasoned arguments for these assumptions, and more precise statements of them, are given in Section 2.2. Both Sections 2.1 and 2.2 are somewhat technical and might be skipped on a first reading of the paper, especially by non-specialists. However, we feel it is much clearer to lay out these assumptions coherently in advance, rather than introducing them piecemeal at various points during the calculations.

2.1 Overview of Technical Difficulties

The first technical challenge is the interpretation of the Doi-Peliti action, whose final (shifted) form is given in Eq. 29 below. The Doi-Peliti field formalism involves a coherent state path integral directly built from the master equation, where the primary fields of the theory are not direct particle densities but conjugate creation and annihilation operators. For this reason, physical observables such as the two-point correlation functions of active and passive particles are typically sums of terms that may scale differently [28]. Based on a Fokker-Planck equation [29], the Doi-Peliti formalism incorporates diffusion and diffusive noise differently compared to the response field formalism based on a Langevin equation of the particle densities. While the former contains a single squared gradient term representing the (stochastic) diffusion, the latter introduces a deterministic squared gradient as well as a conserved noise, which is multiplicative in general [30]. We will argue later that this diffusive noise is potentially dangerously irrelevant.

Both in understanding the physical noise implemented by the Doi-Peliti action, and in calculating the observables, problems arise if these are interpreted from a response-field perspective that does not respect the nature of the fields [22, 31] or ignores their commutator relations [32]. However, as long as the field-theoretic RG machinery in the Doi-Peliti formalism is strictly followed, perturbative RG on it is known to be capable of producing correct exponents for important universality classes. Examples include directed percolation [1, 19] and branching random walks [21]. Such calculations are unambiguous either because there are only a few relevant couplings throughout the RG calculations, or because some type of Ward identity links couplings into a small number of combinations which then flow in lock-step. However, the third of our technical challenges is that more generally (including for RO), there is a plethora of relevant couplings, present in the bare action or potentially generated at the fixed point, which might in principle contribute. To study the RO universality class, extreme care is then needed to preserve the symmetries between couplings (including but not limited to conservation of total particle number) so that the fixed point calculated through the RG analysis is indeed that of RO, rather than some other two-species reaction-diffusion model with, typically, an upper critical dimension of 6 instead of 4 [33, 34].

An additional complication, closely related to the one just outlined, is that there are more relevant parameters in the bare theory than the final effective one. This means that the concept of an RG fixed point has to be replaced by that of an RG fixed-point manifold (FPM). Any point on this manifold is a fixed point of the RG flow functions. This differs from the critical manifold, which is a higher dimensional manifold of starting parameters that flow under RG to the RO FPM (in the Wilsonian RG sense). The FPM is also referred to as a 'class of equivalent fixed points' and leads to redundant operators that do not follow scaling relations nor enter the RG flow functions [35]. Therefore, choosing a judicious form of the fixed point action where many operators are 'redundant' can ease the perturbative RG calculations considerably and we exploit this in our approach below. We discuss the FPM concept further in Appendix B.

Another feature the RO theory is that since passive particles do not diffuse, the passive propagator is momentum-independent. Together with certain generated vertices absent in the bare action, this leads to loop diagrams that exhibit algebraic (not logarithmic) divergences both in the IR and UV regime. Examples of such super-divergent loops will be discussed later and are presented in Appendix C.

Algebraic (not logarithmic) divergences in the IR regime can arise when there is one or more unstable direction leading away from the RO fixed point (with $d_c = 4$) to a generic reaction-diffusion one (with $d_c = 6$). The role of these divergences can be understood by looking at the tricritical fixed point in the Ising model [36]. There, working near the tricritical fixed point, one encounters divergences that would be individually algebraic and are inversely proportional to the mass (distance away from criticality). These are caused by an unstable

direction leading from the tricritical fixed point to the critical (Wilson-Fisher) one which has higher upper critical dimension ($d_c = 4$ rather than $d_c = 3$ for the tricritical point). They cancel when the tricritical fixed point is approached along a path that has no component in the unstable direction and therefore does actually arrive at the fixed point one is trying to study [36]. We will assume below that the same happens in RO.

Algebraic UV divergences arguably pose a bigger and more serious problem. The most rigorous method to resolve such divergence issues is to explicitly show that all algebraic divergences across all relevant couplings cancel, for example by constantly observing certain Ward identities/symmetries between the large number of couplings in order to stay in the RO class. While proving this cancellation explicitly is beyond the scope of the present work, we shall assume that RO cast into a Doi-Peliti field theory is perturbatively renormalisable. A direct consequence of this assumption is that cancellations have to occur for all couplings of this non-renormalisable 'problematic' type that may be generated at the fixed point. Therefore, assuming renormalisability of our theory is enough to ensure that all the problematic couplings, whose bare values are zero in RO, must remain suppressed via cancellations both in the judicious form of the fixed point action and throughout the RG calculations.

So far, exploiting the degeneracy provided by the FPM and the perturbative renormalisability assumption, we have argued that a sensible starting point action of the RG calculations exists. However, there remains a final risk concerning the treatment of vertices that may be generated at the fixed point but not present in the bare theory, which can be crucial to finding the correct exponents. One example of such a scenario is the Fredrickson-Andersen (FA) model [37], where a linear diffusion term is absent in the microscopic description. Though only generated during the flow, the theory without a diffusion term is fundamentally incomplete even at Gaussian level and hence in $d > d_c$. The generated relevant coupling therefore has to be manually put into the starting point action at $O(\epsilon^0)$; without it, the Gaussian starting point is not within $O(\epsilon)$ proximity of the final effective action of the nonlinear model in $d < d_c$, and the resulting theory certainly fails to be perturbatively renormalisable. Correspondingly, the diffusive coupling in FA, once added to the bare theory, must be treated just like the $O(1)$ couplings already present there, so it changes the values of loops used to calculate exponents at $O(\epsilon)$. In making such manual modifications of the action, however, one has to be mindful to not break symmetries, as this could lead to a theory outside the intended universality class. Indeed this was shown for FA [38], which explained why earlier work on that model appeared to give $d_c = 4$ when in fact $d_c = 2$. For this reason, in problems of this type, it is not appropriate to add all relevant terms in the initial action, even if not present already there, purely as a precaution against these being generated at the fixed point. Specifically, one should not add couplings that create algebraic (not logarithmic) divergences near $d_c = 4$ because these generically perturb the RO theory into one with $d_c > 4$.

We can summarize our approach to the apparent divergences as follows. At the RG fixed point of the RO theory, certain problematic couplings (such as the ones exhibited in Appendix C) may be generated, producing loop diagrams with algebraic (not logarithmic) IR and UV divergences. We assume that the Gaussian theory without these couplings makes sense *and* that the nonlinear theory is renormalisable, indicating that these couplings must cancel and can safely be suppressed. A more precise statement of this and other assumptions follows below.

2.2   Statement of assumptions used for the RG calculations

In this Section, we gather the various arguments and assumptions needed to overcome the technical difficulties surveyed above, so that our perturbative RG calculations can give unambiguous exponent predictions at order ϵ.

1. *Universality*

   (a) We consider the Random Organization (RO) model where a non-conserved order parameter (ρ_A) is coupled to a conserved density (ρ), and can undergo absorbing state phase transitions into infinitely many absorbing state configurations. We **argue** that this describes a large universality class, which we hereafter refer to as the RO class. A minimal realization is a reaction-diffusion system consisting of an 'active' diffusing species (diffusivity D) and a 'passive' non-diffusing species, with number-conserving reactions $A \rightarrow P$ and $A + P \rightarrow A + A$. The intrinsic noise in the Doi-Peliti theory, when written in terms of Langevin equations, include both a birth-and-death, multiplicative noise $\sim \sqrt{\rho_A}\eta$, and a diffusive, conserved noise $\sim \sqrt{D\rho_A}\nabla \cdot \Xi$. Here η and Ξ are Gaussian white spatiotemporal noises of suitable dimensionality.

   (b) The RO class we propose differs from the customary C-DP/Manna/q-EW class by including the diffusive conserved noise. Since this term is RG-irrelevant, we **argue** that the RO universality class has the same upper critical dimension $d_c = 4$ as C-DP/Manna/q-EW, and shares the same order parameter exponent β, dynamic exponent z, and correlation length exponent $\nu_\perp$.

   (c) We **argue** that the diffusive noise, despite its RG-irrelevance, can alter the hyperuniformity exponent describing total density correlation functions, because it is *dangerously* irrelevant. This can create an important distinction between RO and C-DP/Manna, while leaving $\beta, z, \nu_\perp$ and d_c equal for the two classes. We elaborate this reasoning further in Sections 3.3 and 5.2 below. In particular we **define** the RO class to exclude cases where the particles move only by centre-of-mass-conserving interactions, such as those considered in [26], whose additional conservation law eliminates the diffusive noise.

   (d) We **argue** that, because of the presence of more relevant parameters in the bare theory than in the final effective one, the concept of an RG fixed point has to be replaced by that of an RG fixed-point manifold (FPM); see Appendix B for details. We **assume** that any microscopic theory that flows to the shared FPM under RG is a member of the RO universality class.

2. *Renormalisability*

   (a) We **assume** that the Doi-Peliti theory for RO is renormalisable around its upper critical dimension $d_c = 4$.

   (b) Given this and 1d above, we **argue** that starting at a point on the Gaussian FPM, in $d = 4 - \epsilon$ the renormalised nonlinearities corresponding to a microscopic theory in the RO class will generically correspond to a fixed point somewhere on RO's FPM in the IR limit, which we **assume** is in $\mathcal{O}(\epsilon)$ vicinity of the Gaussian FPM. This allows us to study the fixed point governed by a particular microscopic action rather than one containing all possible relevant terms.

   (c) Within a general reaction-diffusion setting there are many nonlinearities that violate the main precept of RO and/or C-DP classes (namely, an infinite number of absorbing states that are not symmetry-related). For the generality of these models d_c is not 4 but 6. Such terms enter our initial action for RO in specific combinations. Yet taken individually, each can generate problematic, algebraic (not logarithmic) divergences in $d = 4$ which we **argue** (given that $d_c = 4$, see assumption 1b above) must cancel.

(d) We **assume** that this cancellation follows a broadly similar scenario to that for the equilibrium tricritical Ising model ($d_c = 3$), at least in the IR regime.

3. *Hyperuniformity*

We **assume** that the spatial correlations in total density are hyperuniform at criticality in RO. This assumption is supported by simulation data [8,9]. It not necessary for determining z, $\nu_\perp$, or any other critical exponents that can be found via scaling relations from these two. It is however needed to extract β (to order ϵ), as well as the hyperuniformity exponent ς, from our perturbative RG approach. We refer to Section 5 for a discussion of the numerical evidence and of further implications of this assumption.

3 The Gaussian Theory

We now study the RO universality class at Gaussian level, starting from a particular microscopic realization.

3.1 Field Theory

We consider a lattice model comprising A particles that hop with diffusivity D and non-hopping P particles. The on-site reaction $A + P \rightarrow 2A$ has rate κ, causing passive particles to awaken on encounter with active ones; the reaction $A \rightarrow P$ has rate μ so that active particles decay to passivity without collisions. Following established procedures [19,39] we start by writing the master equation for the model. Letting n_i denote the number of active particles at position i and m_j the number of passive particles at position j, the master equation is

$$\partial_t P(n, m, t) = \mu \sum_i \Big((n_i + 1) P(n + 1_i, m - 1_i, t) - n_i P(n, m, t) \Big)$$
$$+ \kappa \sum_i \Big((n_i - 1)(m_i + 1) P(n - 1_i, m + 1_i, t) - n_i m_i P(n, m, t) \Big) \qquad (1)$$
$$+ \frac{D}{h^2} \sum_{\langle i,j \rangle = h} \Big((n_j + 1) P(n + 1_j - 1_i, m, t) - n_i P(n, m, t) \Big)$$

Here n and m are shorthands for the collections of all n_i and m_j respectively, and where 1_i is used to add or subtract a single particle at position i; h is the distance between neighbouring sites and $\langle i, j \rangle = h$ sums over all neighbours. In terms of annihilation operators $\hat{\mathbf{a}}, \hat{\mathbf{p}}$ and creation operators $\hat{\mathbf{a}}^\dagger, \hat{\mathbf{p}}^\dagger$ for A and P particles respectively, and via a coherent-state path integral and the continuum limit [19], we derive a Doi-Peliti action $\mathcal{A} = \int \mathbb{A} \, d^d x \, dt$ with Lagrangian density

$$\mathbb{A} = -a^\dagger (\partial_t - D\nabla^2) a - p^\dagger \partial_t p + \mu(p^\dagger - a^\dagger)a + \kappa a^\dagger (a^\dagger - p^\dagger)ap \qquad (2)$$

where site- and time-indices are suppressed to ease notation. Notably, the action density observes a $U(1)$ symmetry, since it remains invariant under multiplication of the creation fields by a phase factor $e^{i\psi}$ and the annihilation fields by $e^{-i\psi}$ for any real number ψ. The conserved charge corresponding to this symmetry is exactly the total number conservation.

Upon performing the Doi shift $\hat{\mathbf{a}}^\dagger = \tilde{\mathbf{a}} + 1, \hat{\mathbf{p}}^\dagger = \tilde{\mathbf{p}} + 1$, the action density becomes

$$\mathbb{A} = -\tilde{a}(\partial_t - D\nabla^2)a - \tilde{p}\partial_t p + \mu(\tilde{p}a - \tilde{a}a) + \kappa(\tilde{a}^2 ap + \tilde{a}ap - \tilde{a}a\tilde{p}p - a\tilde{p}p) \qquad (3)$$

in terms of the fields $a(x,t), \tilde{a}(x,t), p(x,t), \tilde{p}(x,t)$, where we have used bold symbols to denote operators and plain symbols for fields, and the arguments of the fields in the above expression have been suppressed for clarity. While the Doi shift disguises the $U(1)$ symmetry, a consequence which could potentially lead to symmetries being overlooked [40], we keep track of the associated particle conservation and use the Doi-shift to conveniently cancel undesired sink-terms, that appear as surface terms in the construction of the field theory or as additional terms in the master equation implementing spontaneous extinction.

At mean-field level, we identify the active particle annihilation field that minimises the action with the mean-field density ρ_A, and the minimising passive particle annihilation field with ρ_P. This gives the expected equations of motion for the global densities at mean-field level, $\dot{\rho}_A = -\mu\rho_A + \kappa\rho_P\rho_A$ and $\dot{\rho} = 0$.

The spatially averaged total density of active and passive particles $\rho = \rho_A(t) + \rho_P(t)$ does not evolve in time, and acts as a control parameter of the system. When ρ is larger than a critical value $\rho_c = \mu/\kappa$, there are two stationary solutions to the mean-field equations: an unstable one where $\rho_A = 0$ (the absorbing state), and the other stable solution with $\rho_A = (\rho - \rho_c)^1 > 0$, $\rho_P = \rho_c$. Thereby the well-established mean-field critical exponent $\beta = 1$ [2] is confirmed. At mean-field level, the system stays in the active phase indefinitely whenever $\rho > \rho_c$. Meanwhile for $\rho < \rho_c$, the only stable solution is $\rho_A = 0$, and the system is in the absorbing phase.

3.2 Gaussian Structure Factors: Hyperuniformity via Anticorrelation

Next we expand (3) about the mean field solution and shift $a(x,t) = a_0 + \breve{a}(x,t)$ and $p(x,t) = p_0 + \breve{p}(x,t)$ [20]. These shifts should not be simply interpreted as perturbations away from mean densities (particularly as annihilation fields in Doi-Peliti formalisms are *not* exactly mapped to actual particle densities); rather, a_0 and p_0 are the mean densities of a set of *Poisson-distributed* active and passive particles *initialised in the distant past* [32]. Using active particles as an example, an a_0-Poisson distribution at site i can be initialised at time t_0 at the operator level:

$$|\mathcal{M}(t_0)\rangle = e^{-a_0}\sum_{l=0}^{\infty}\frac{a_0^l}{l!}|l_i,0\rangle = e^{-a_0}\sum_{l=0}^{\infty}\frac{a_0^l \hat{\mathbf{a}}_{\mathbf{i}}^{\dagger l}}{l!}|0,0\rangle \tag{4}$$

This initialisation can be applied at every position and in order to shorten the notation, we drop the subscript i.

If the expectation of an observable $\mathcal{O}$ is evaluated at time $t_1 > t_0$, the initialisation can be compactly written as an additional term that is added to the action (at the field level):

$$\left\langle \mathcal{O}(t_1)e^{-a_0}\sum_{l=0}^{\infty}\frac{a_0^l a^{\dagger l}(t_0)}{l!}\right\rangle = \int \mathcal{D}[\tilde{a},a]\mathcal{O}(t_1)e^{\mathcal{A}+a_0(a^{\dagger}(t_0)-1)}$$
$$= \int \mathcal{D}[\tilde{a},a]\mathcal{O}(t_1)e^{\mathcal{A}+a_0\tilde{a}(t_0)} \tag{5}$$

This additional term can be absorbed by shifting the annihilation field by a_0 from time t_0 onwards, $a(x,t) = \breve{a}(x,t) + a_0\Theta(t - t_0)$: in the propagator, $-\tilde{a}(x,t)\partial_t a(x,t)$ is replaced by $-\tilde{a}(x,t)\partial_t\breve{a}(x,t) - a_0\tilde{a}(x,t)\delta(t - t_0)$. Integrated in time, the second term becomes $-a_0\tilde{a}(t_0)$, hence cancelling the extra term created by the initialisation in (5). We then push back the initialisation time $t_0 \to -\infty$ which makes the Heaviside function $\Theta(t - t_0)$ obsolete.

The fact that the initialisation is pushed back to $t_0 \to -\infty$ implies that, if left unperturbed, the system is in steady state at any finite time t. In this Section we do leave the system unperturbed after the initialisation at $t_0 = -\infty$, and the only observables that we calculate are the correlators for the various particle types.

At Gaussian (linear) level, the passive particle density converges to the critical (total) density $\rho_{c,g} = \mu/\kappa$, where $\rho_{c,g}$ carries the suffix g to indicate that it is the bare Gaussian value of the critical density, and the active particle density converges to $\rho - \rho_{c,g}$, together conserving total particle number. Consequently, if we initialise with Poisson-distributed passive density $p_0 = \rho_{c,g} = \mu/\kappa$ and $a_0 = \rho - \rho_{c,g}$, the large-time limits of active and passive densities remain unchanged from their initial mean values. In particular, $a_0 = 0$ identifies the critical point at the Gaussian level; crucially, this feature of the Gaussian model will change in Section 4 below for the nonlinear theory. The quadratic part of the Lagrangian of the Doi-Peliti theory is thereby found as[1]

$$\mathbb{A}_{G,DP} = -\tilde{a}(\partial_t - D\nabla^2)\breve{a} - \tilde{p}(\partial_t + \kappa a_0)\breve{p} + \kappa a_0 \tilde{a}\breve{p} + \kappa a_0 p_0(\tilde{a}^2 - \tilde{a}\tilde{p}) \tag{6}$$

Propagators can be read off from here, but as already discussed in Section 2.1, in Doi-Peliti theory there is a nontrivial relation between terms in the action and the physical densities and noises [19, 39]. This means that calculating static density correlators $S_{\alpha\beta}(q)$ for $\alpha, \beta \in A, P$ requires a tree-level computation.

The particle number operator $\hat{\rho}_{\mathbf{A}} := \hat{\mathbf{a}}^\dagger \mathbf{a}$ is translated to $\langle \rho_A(x,t) \rangle = \langle a^\dagger(x,t)a(x,t) \rangle$ at the field level. The covariance in spatial Fourier space and temporal direct space between active particle densities is calculated in Doi-Peliti field theory as

$$\begin{aligned}
\langle \rho_A \rho_A' \rangle &= \langle a^\dagger a a'^\dagger a' \rangle = \langle a a'^\dagger a' \rangle = \langle a\tilde{a}'a' \rangle + \langle a a' \rangle \\
&= a_0^2 + a_0 \langle \breve{a} \rangle + a_0 \langle \breve{a}' \rangle + \langle \breve{a}\tilde{a}' \rangle + a_0 \langle \breve{a}\tilde{a}' \rangle + \langle \breve{a}\tilde{a}'\breve{a}' \rangle
\end{aligned} \tag{7}$$

where a prime indicates that the field has arguments $(-q, t')$, whereas without the prime the field has arguments (q, t) in spatial Fourier space. From this point onward, we will remain at the field level rather than the operator level, and this shorthand notation for arguments will be used consistently. Then,

$$\begin{aligned}
\delta^d(q + q')\text{Cov}[\rho_A, \rho_A'] &= \langle \rho_A \rho_A' \rangle - \langle \rho_A \rangle \langle \rho_A' \rangle \\
&= a_0^2 + a_0 \langle \breve{a} \rangle + a_0 \langle \breve{a}' \rangle + \langle \breve{a}\tilde{a}' \rangle + \\
&+ a_0 \langle \breve{a}\tilde{a}' \rangle + \langle \breve{a}\tilde{a}'\breve{a}' \rangle - (a_0 + \langle \breve{a} \rangle)(a_0 + \langle \breve{a}' \rangle) \\
&= a_0 \langle \breve{a}\tilde{a}' \rangle + \langle \breve{a}\tilde{a}' \rangle - \langle \breve{a} \rangle \langle \breve{a}' \rangle + \langle \breve{a}\tilde{a}'\breve{a}' \rangle
\end{aligned} \tag{8}$$

This expression confirms our statement in Section 2.1 that the correlators involves sums over several scaling fields of the theory, so that to find their scaling one has to see which terms dominate on the right hand side.
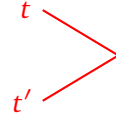
At Gaussian level, the third and fourth terms in (8) give zero contributions, since these rely on 'source vertices' (these are couplings $\tilde{a}$, $\tilde{p}$, contributing to $\langle \breve{a} \rangle$, $\langle \breve{p} \rangle$ at tree-level, e.g. $\langle \breve{a} \rangle = \underline{\hspace{1cm}}\times$), which retain values of zero in the Gaussian theory. Up to the prefactor a_0, the first term equals the propagator, which can be read off from the quadratic part of the action in Fourier space

$$\langle \breve{a}(q,t)\tilde{a}(-q,t') \rangle = \delta^d(0) \int \frac{e^{-i\omega(t-t')}}{-i\omega + Dq^2} d\omega \tag{9}$$

where the formal factor $\delta^d(0)$ equates to the volume of the system (this factor will also arise in Equations (10)–(17) below). Meanwhile the second contribution $\langle \breve{a}\tilde{a}' \rangle$ in (8) can be calculated
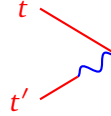
---

[1]Notably, while in the original action (3) the passive propagator is singular since it does not contain any diffusion or mass term, the passive propagator in (6) after performing the shifts a_0 and p_0 attains a mass term. This regularises the infrared divergences.

in Fourier space as the sum of two Feynman diagrams, using standard rules for calculating such observables. The diagrams are

$$
\kappa p_0 a_0 \;\hat{=}\; \delta^d(0) \int \frac{2\kappa p_0 a_0 e^{-i\omega(t-t')}}{(-i\omega + Dq^2)(i\omega + Dq^2)} d\omega \tag{10}
$$

where the factor of 2 comes from the symmetry factor of the active-active noise vertex, and

$$
-\kappa p_0 a_0 \;\hat{=}\; -\delta^d(0)\,\kappa p_0 a_0 \int \frac{e^{-i\omega(t-t')}\kappa a_0}{(-i\omega + Dq^2)(i\omega + Dq^2)(i\omega + \kappa a_0)} d\omega \tag{11}
$$

which appears on the right-hand side of (8) once in this form and once with dashed and undashed variables interchanged.

Adding these contributions together and taking the inverse temporal Fourier transform gives the active-active covariance at wavevector q as

$$
\mathrm{Cov}[\rho_A(q,t), \rho_A(-q,t')] = a_0\left(e^{-Dq^2|t-t'|} + \kappa p_0 \frac{Dq^2 e^{-Dq^2|t-t'|} - \kappa a_0 e^{-\kappa a_0|t-t'|}}{(Dq^2 + \kappa a_0)(Dq^2 - \kappa a_0)} \right) \tag{12}
$$

Similarly the passive-passive covariance equals

$$
\delta^d(q+q')\mathrm{Cov}[\rho_P, \rho_P'] = p_0\left\langle \breve{p}\tilde{p}' \right\rangle + \left\langle \breve{p}\breve{p}' \right\rangle - \left\langle \breve{p} \right\rangle \left\langle \breve{p}' \right\rangle + \left\langle \breve{p}\tilde{p}'\breve{p}' \right\rangle \tag{13}
$$

Since there is no tree-level diagram that represents a two-point passive-passive noise vertex, contributions like $\langle \breve{p}\breve{p}' \rangle$ on the right hand side are zero. The only contributing part is the first term, which is the passive propagator multiplied by p_0; hence we directly obtain

$$
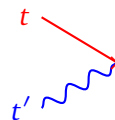\mathrm{Cov}[\rho_P(q,t), \rho_P(-q,t')] = p_0 e^{-\kappa a_0|t-t'|} \tag{14}
$$

Finally, the active-passive covariance is calculated as follows

$$
\delta^d(q+q')\mathrm{Cov}[\rho_A, \rho_P'] = \Theta(t-t')\left(\langle \breve{a}\tilde{p}'\breve{p}' \rangle + p_0\langle \breve{a}\tilde{p}' \rangle \right) + \Theta(t'-t)\left(\langle \breve{p}'\tilde{a}\breve{a} \rangle + a_0\langle \breve{p}'\tilde{a} \rangle \right) + \langle \breve{a}\breve{p}' \rangle - \langle \breve{a} \rangle \langle \breve{p}' \rangle \tag{15}
$$

This has contributions from 'transmutation', whose propagator connects the two species

$$
\langle \breve{a}(q,t)\tilde{p}(-q,t') \rangle = \delta^d(0) \int \frac{\kappa a_0 e^{-i\omega(t-t')}}{(-i\omega + Dq^2)(-i\omega + \kappa a_0)} d\omega \tag{16}
$$

and from the active-passive noise vertex,

$$
-\kappa p_0 a_0 \;\hat{=}\; \delta^d(0)\kappa p_0 a_0 \int \frac{-e^{-i\omega(t-t')}}{(-i\omega + Dq^2)(i\omega + \kappa a_0)} d\omega \tag{17}
$$

When combined and inverse Fourier transformed in time, these give

$$
\mathrm{Cov}[\rho_A(q,t), \rho_P(-q,t')] = \Theta(t-t')\frac{\kappa a_0 p_0}{Dq^2 - \kappa a_0}\left(e^{-\kappa a_0|t-t'|} - e^{-Dq^2|t-t'|} \right)
$$
$$
- \kappa p_0 a_0 \frac{\Theta(t-t')e^{-Dq^2|t-t'|} + \Theta(t'-t)e^{-\kappa a_0|t-t'|}}{(Dq^2 + \kappa a_0)} \tag{18}
$$

Adding all three covariances together, we obtain finally the covariance for the total density $\rho(x, t) = \rho_A(x, t) + \rho_P(x, t)$ as

$$\text{Cov}[\rho(q, t), \rho(-q, t')] = a_0 e^{-Dq^2|t-t'|}\left(1 - \frac{Dq^2\kappa p_0}{(Dq^2 + \kappa a_0)(Dq^2 - \kappa a_0)}\right) + p_0 e^{-\kappa a_0|t-t'|}\left(\frac{(Dq^2)^2}{(Dq^2)^2 - (\kappa a_0)^2}\right)$$

(19)

Taking $t = t'$ gives the equal-time structure factor,

$$S(q) = a_0 + p_0 \frac{Dq^2}{Dq^2 + \kappa a_0} = a_0 + p_0 \frac{(q\xi)^2}{1 + (q\xi)^2}$$

(20)

where $\xi = \sqrt{D/(\kappa a_0)} \sim (\kappa a_0)^{-1/2}$ is the correlation length. This confirms the mean-field critical exponent $\nu = 1/2$. The critical point is at $a_0 \propto \xi^{-2} \to 0$. This implies vanishing of $S(0)$, and hence hyperuniformity, so long as the $q \to 0$ limit is taken first, whereas for finite q, $S(q)$ approaches a constant, p_0, as $a_0 \to 0$. Therefore at criticality $S(q)$ is zero at the origin but p_0 elsewhere, which can be formally viewed as $S(q) \sim q^\varsigma$ with exponent $\varsigma = 0^+$. Note, however, that this order of limits formally reverses the one used in RG to access the critical scaling.
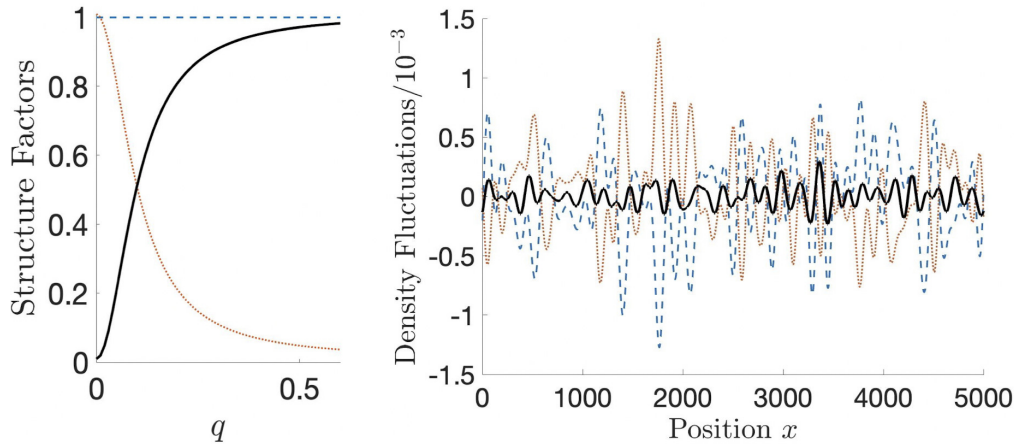

Figure 1:   (a) Plot of structure factors $S(q), S_{AA}(q), S_{PP}(q)$ vs q for $a_0 = 0.01, p_0 = \kappa = D = 1$ (giving $\xi = 10$) showing at low q the cancellation-induced suppression of total density fluctuations. Blue dashed line (horizontal) passive; red dotted line (decreasing) active; black solid line (increasing) total density. (b) Sample of spatial density statistics for the Gaussian model in $d = 1$. Parameters as for (a); bold black line is the total density.

Fig. 1 shows the three structure factors, and sampled density profiles (in $d = 1$ for simplicity), at small a_0. This strikingly demonstrates how hyperuniformity emerges by anticorrelation of passive and active particles. This must be so, because the $S_{AA,PP}(0)$ correlators found above each remain finite at criticality ($a_0 \to 0$), where the full density has $S(0) = 0$. While the Gaussian-level calculation does not enforce separate positivity of the cancelling particle densities ρ_A and ρ_P, we show later (Section 5) that doing so requires strong non-Gaussianity only in dimension $d < d_c = 4$.

In the RO theory constructed from the Doi-Peliti formalism, there is no unique fixed point action, with couplings replaced by their renormalised values at the RG fixed point, but a *manifold* of fixed point actions (the FPM). This is since each reaction gives rise to more coupling constants than there are independent *effective* coupling constants, and degeneracy of the 'fixed

point action' arises. While the detailed discussion for the FPM is left to Appendix B, we now briefly show this degeneracy in $d > 4$ dimensions for the Gaussian theory. Here, the perturbative terms (terms not in the harmonic part) of the RO model constructed from any subset of allowed reactions are zero for any fixed point on the Gaussian FPM, and what remain are purely quadratic terms that only follow engineering dimensions. Therefore, the conventionally defined 'fixed point action' of the Gaussian theory is simply the Gaussian part of the original action, with values $\alpha_1, \alpha_2, \alpha_3$ given by the microscopic reactions chosen (examples below):

$$\mathbb{A} = -\tilde{a}(\partial_t - D\nabla^2)\breve{a} - \tilde{p}(\partial_t + \tau_p)\breve{p} + \tau_p \tilde{a}\tilde{p} + \alpha_1 \tilde{a}^2 + \alpha_2 \tilde{a}\tilde{p} + \alpha_3 \tilde{p}^2 \qquad (21)$$

- For reactions $\{A \to P, A + P \to A + A\}$, $\alpha_3 = 0$ in the Gaussian fixed point action.

- For reactions $\{A \to P, A + P \to A + A, A + A + P \to A + P + P\}$, all three α terms are present in the Gaussian fixed point action. Note that although RG-relevant, the last of these reactions does not change the universality class.

The resulting Gaussian exponents do not differ, despite being calculated from different Gaussian fixed point actions. For example, the total density correlator obeys

$$\mathrm{Cov}[\rho(q,t)\rho(-q,t)] = a_0 + p_0 - \frac{\alpha_1}{Dq^2 + \tau_p} + \frac{\alpha_3}{\tau_p} + (\alpha_1 + \alpha_2 + \alpha_3)\frac{1}{Dq^2} = \frac{\alpha_1}{Dq^2 + \tau_p} + \frac{\alpha_3}{\tau_p} \quad (22)$$

where in the last step we have exploited the symmetry $\alpha_1 + \alpha_2 + \alpha_3 = 0$ specific to the RO class; this will be proved in Section 4.3. In particular, this symmetry is exactly what ensures the Gaussian RO fixed point to exhibit hyperuniform, not diverging, fluctuations in total density. This exemplifies for the Gaussian case how a degeneracy of the fixed point action arises (here between the values of $\alpha_{1,2,3}$). Importantly, for $d > d_c = 4$, not all relevant parameters have to be present in the initial action for RG to give the correct exponents, as long as the one starts on the correct (Gaussian RO) fixed-point manifold.

3.3 Hyperuniformity and Conservative Noise at Gaussian Level

A further aspect of the Gaussian theory is exposed by using the Cole-Hopf transformation [39] to find the equivalent Langevin equations, from which the same structure factors as found above can alternatively be derived.

In response field formalisms, annihilation fields in the action represent real density fields, conjugated with artificial creation fields. Averaging over the white noise in the Langevin equations through completing the square shows that quadratic terms in the creation fields represent the statistical weight of the action (details of this derivation can be found in Chapter 4.1 in [19]). However, naively applying the same derivation to Doi-Peliti often yields imaginary noise in reaction-diffusion systems, including RO [15]. This is because, in Doi-Peliti field theory, the annihilator field is the complex conjugate of the creator field, whereas they are independent in the response field formalism. Only in the latter can anything be integrated out at all without carrying out the whole path integral.

This problem is overcome by a Cole-Hopf transformation [39], creating a response-field dual of the Doi-Peliti action, in order to obtain an action in terms of active and passive particle density fields, α and π, and their response fields $\tilde{\alpha}$ and $\tilde{\pi}$. Here

$$a = \exp(-\tilde{\alpha})\alpha \qquad a^\dagger = \exp(\tilde{\alpha}) \qquad (23a)$$

$$p = \exp(-\tilde{\pi})\pi \qquad p^\dagger = \exp(\tilde{\pi}) \qquad (23b)$$

Notice that the dual annihilation field obeys $\alpha = a^\dagger a$ and so represents a real density. Again performing a shift $\alpha \to \alpha + \alpha_0$ and $\pi \to \pi + \pi_0$ and keeping only the quadratic parts, the

Cole-Hopf action for RO is at Gaussian level

$$\mathbb{A}_{G,CH} = -\tilde{\alpha}\partial_t\alpha + D(-\nabla\tilde{\alpha}\nabla\alpha + (\nabla\tilde{\alpha})^2\alpha_0) - \tilde{\pi}\partial_t\pi + \kappa(\tilde{\alpha}-\tilde{\pi})\alpha_0\pi + \mu(\tilde{\alpha}-\tilde{\pi})^2\alpha_0 \qquad (24)$$

There are two advantages of this Cole-Hopf action. Firstly, since α and π are particle density fields, the active density correlator can be written neatly as $\langle\alpha\alpha\rangle$, in contrast to (8). (Likewise the other density correlators also.) Therefore calculations of correlation functions at tree-level are more straightforward. In particular, Feynman diagrams reduce to the noise-vertex ones, such as (10), and do not include propagators such as (9). Secondly, it is now possible to use a response-field formalism to derive the corresponding real noises in the Langevin equations: the quadratic terms in the creation fields, $\mu(\tilde{\alpha}-\tilde{\pi})^2\alpha_0$ and $D(\nabla\tilde{\alpha})^2\alpha_0$, represent two noises respectively. Starting with the first of these, then since

$$e^{\int dt d^d x\,\mu\alpha_0(\tilde{\alpha}-\tilde{\pi})^2} \propto \int d\eta\, e^{\int dt d^d x\,(\tilde{\alpha}-\tilde{\pi})\eta - \eta^2/(4\mu\alpha_0)} \qquad (25)$$

we recover a birth-and-death noise $\sqrt{2\mu a_0}\eta$ in the Langevin equation for ρ_A, and $-\sqrt{2\mu a_0}\eta$ in the Langevin equation for ρ_P, with η unit white Gaussian noise. These two noises are equal and opposite, so there is no birth-and-death noise in the Langevin equation for the total density ρ. This must indeed be the case to conserve the total particle number. For the second term, notice that

$$e^{\int dt d^d x\,D\alpha_0(\nabla\tilde{\alpha})^2} \propto \int d\Xi\, e^{\int dt d^d x\,\Xi\cdot\nabla\tilde{\alpha} - \Xi^2/(4D\alpha_0)} \qquad (26)$$

where Ξ is unit white vectorial noise. Using integration by parts on the term $\Xi\cdot\nabla\tilde{\alpha}$, we find an additional conserved noise $\sqrt{2Da_0}\nabla\cdot\Xi$ in the Langevin equation for ρ_A. We note that a rigorous derivation of the nonlinear Langevin equations from the Doi-Peliti fields (i.e. without using Cole-Hopf transformation) can be performed using contour deformations in the complex plane [31].

Summarising the above, the Langevin equations *at Gaussian level* read

$$\frac{\partial\rho_A}{\partial t} = D\nabla^2\rho_A - \mu\rho_A + \kappa a_0(\rho - \rho_A - p_0) + \sqrt{2\mu a_0}\eta + \sqrt{2Da_0}\nabla\cdot\Xi \qquad (27)$$

$$\frac{\partial\rho}{\partial t} = D\nabla^2\rho_A + \sqrt{2Da_0}\nabla\cdot\Xi \qquad (28)$$

Here η and Ξ are unit white Gaussian noises as stated above. The variance for the noises are proportional to a_0 and not ρ_A since multiplicative noises become additive at the Gaussian level. Directly solving for the equal-time structure factor from (27,28) confirms our result (20). This agreement of results demonstrates field-level Cole-Hopf transformation as a good heuristic for deriving Langevin equations from Doi-Peliti actions. However, it is important to note that operator-level Cole-Hopf is invalid, as it would wrongly suggest that the annihilation operator is invertible, and that truncating the Cole-Hopf action at quadratic order also lacks clear justifications. Therefore, we restrict the application of Cole-Hopf transformation to Gaussian level.

Moreover one also finds that without the diffusive noise Ξ, the a_0 term in (20) is absent: hyperuniformity (now with $\varsigma = 2$) then also arises at $\xi < \infty$, that is, *away from criticality*. Thus, discarding diffusive noise alters the Gaussian-level predictions dramatically, although it is often discarded for C-DP and, by extension, RO on the basis that it is irrelevant in the RG sense [6, 15, 22]. Irrelevant variables that change correlation functions are known in the literature as *dangerously irrelevant* [23]. We return to this point in the RG setting for $d < 4$, in Section 5.2 below.

Meanwhile, our finding of an exponent $\varsigma = 2$ throughout the active phase matches results for particles with RO- or C-DP-like interactions in which the centre of mass of the density

field is conserved [26]. This arises if particles move only by pairwise events in which the two particles are displaced by equal and opposite amounts [26]. Notably, without noise, (28) has an equivalent conservation law, as follows. The 'mass-moment' density field $\mathbf{p} = \rho\mathbf{r}$ obeys $\dot{p}_\alpha = -(\nabla_\beta J_\beta)r_\alpha = -\nabla_\beta(J_\beta r_\alpha) + J_\alpha$. For $\Xi = 0$ only, the current $\mathbf{J} = -D\nabla\rho_A$ in (28) is of pure gradient form, so that $\dot{p}_\alpha = -\nabla_\beta\Sigma_{\beta\alpha}$ with $\Sigma = \mathbf{J}\mathbf{r} + \mathbf{I}D\rho_A$ where $\mathbf{I}$ is the unit tensor. Hence the mass-moment $\int \mathbf{p}d\mathbf{r}$ in any region is conserved unless there are currents Σ across its boundary [41]; for further discussions see [42]. In Section 2.2 we *defined* the RO universality class to exclude cases with this additional conservation law. It is an open question whether and how a Doi-Peliti theory can be constructed for the separate universality class describing the conserved centre-of-mass case, but as mentioned in Section 2.1, there is no simple way to delete the diffusive noise from our Doi-Peliti action for RO.

4 Perturbative Renormalisation Group Analysis

We now move onto the nonlinear theory that prevails in $d < d_c = 4$, working to one loop in perturbation theory or equivalently to first order in $\epsilon = 4 - d$. We mostly follow the standard procedure of using dimensional regularisation in $d = d_c - \epsilon = 4 - \epsilon$ dimensions [19, 43]. We start from an action constructed by a particular subset of allowed reactions, as employed at the Gaussian level in Section 3, that ensure the RO class is being studied. Doing so requires that there exists a critical FPM (degeneracy of fixed point action, assumption 1d in Section 2.2), and that perturbation theory is renormalisable (assumption 2a there).

4.1 The Nonlinear Action and its Scaling Fields

The full nonlinear bare Lagrangian, found after performing the shifts already detailed in Section 3, is

$$\mathbb{A} = -\tilde{a}(\partial_t - D\nabla^2)\breve{a} - \tilde{p}(\partial_t + \kappa a_0)\breve{p} + \kappa a_0 \tilde{a}\breve{p} + \kappa a_0 p_0(\tilde{a}^2 - \tilde{a}\tilde{p})$$
$$+ \kappa p_0(\tilde{a}^2 - \tilde{a}\tilde{p})\breve{a} + \kappa a_0(\tilde{a}^2 - \tilde{a}\tilde{p})\breve{p} + \kappa(\tilde{a} - \tilde{p})\breve{a}\breve{p} + \kappa(\tilde{a}^2 - \tilde{a}\tilde{p})\breve{a}\breve{p} \quad (29)$$

Here, the first line in (29) is the harmonic part of the action and the second line is the perturbative nonlinear part. The bare propagators can be read off from the action as

$$\begin{pmatrix} \langle\breve{a}(q,\omega)\tilde{a}(q',\omega')\rangle & \langle\breve{a}(q,\omega)\tilde{p}(q',\omega')\rangle \\ \langle\breve{p}(q,\omega)\tilde{a}(q',\omega')\rangle & \langle\breve{p}(q,\omega)\tilde{p}(q',\omega')\rangle \end{pmatrix} = \begin{pmatrix} -i\omega + Dq^2 & -\kappa a_0 \\ 0 & -i\omega + a_0\kappa \end{pmatrix}^{-1} \delta^d(q+q')\delta(\omega+\omega')$$

$$= \begin{pmatrix} \frac{1}{-i\omega+Dq^2} & \frac{\kappa a_0}{(-i\omega+Dq^2)(-i\omega+a_0\kappa)} \\ 0 & \frac{1}{-i\omega+a_0\kappa} \end{pmatrix} \delta^d(q+q')\delta(\omega+\omega')$$
$$(30)$$

At the RG fixed point, all relevant coupling constants will be renormalised and therefore can differ from their bare values shown above. Therefore we introduce names for these coupling constants and organize them systematically according to diagram topology. For example, the passive-to-active transmutation coupling will be denoted by τ_p and the passive mass by ϵ_p; both have bare values of κa_0. Similarly the active-to-passive transmutation coupling τ_a has zero bare value as does the active bare mass ϵ_a. We show other couplings diagrammatically in (31) below, using the following (standard) rules for drawing Feynman diagrams in the Doi-Peliti formalism:

- Each annihilation field $\breve{a}$ (or $\breve{p}$) in the calculation of observable $\mathcal{O}$ is represented as a left end point of a leg.

- Each creation field $\tilde{a}$ (or $\tilde{p}$) in the calculation of observable $\mathcal{O}$ is represented as a right end point of a leg.

- Each interaction vertex in the action $\tilde{a}^k \breve{a}^l \tilde{p}^m \breve{p}^n$ is represented by a node with l active propagators and n passive propagators coming from the right, and k active propagators and m passive propagators going out from the left.

- Time flows from right to left, and hence the left-right order of lines must be obeyed in order to respect time ordering.

Drawing active fields as straight red lines and passive fields as blue wavy lines, we can now represent all the remaining interaction vertices present at bare level as amputated Feynman diagrams:

$$\tag{31}$$

Eq. (31) shows all the nonlinear coupling constants and vertices of the bare action. Other coupling constants could in general be generated at the RG fixed point without topological constraints on the corresponding vertices, that is, all vertices involving incoming and outgoing straight and wiggly lines are allowed in principle. However, we show in Sec. 4.3 that various other constraints on coupling constants are important in our theory for RO. Particularly important will be the following three interactions that are absent initially but could be generated at the RG fixed point:

$$\tag{32}$$

These are the vertices that create algebraic divergences as mentioned in Section 2 and Appendix C. Our assumption of renormalisability (2a in Section 2.2) indicates that these vertices must be suppressed beyond bare level via some type of cancellation at the critical RG fixed point.

In terms of a momentum scale $q \sim \zeta^1$, $x \sim \zeta^{-1}$ (as shorthand, we write $[q] = 1, [x] = -1$), one should usually be able to find scaling dimensions for all fields and coupling constants. It should then be possible to find the engineering dimensions of the fields by power counting. However, rescaling of the fields is non-trivial in the RO model: creation and annihilation operators do not necessarily have the same engineering dimensions. These redundant degrees of freedom can sometimes be readily fixed either via symmetries between the annihilation and creation fields (such as rapidity-reversal symmetry present in directed percolation), or through physical arguments that enforce two or more interaction terms to be equally relevant [44].

In our calculations for Gaussian correlators in Subsection 3.2, all Gaussian correlators, including $\langle \breve{a}(q,t)\tilde{a}(-q,t) \rangle$, $\langle \breve{a}(q,t)\breve{a}(-q,t) \rangle$, $\langle \breve{a}(q,t)\breve{p}(-q,t) \rangle$ and $\langle \breve{p}(q,t)\breve{p}(-q,t) \rangle$, scale as $q^0 F(q\xi)$ at bare level. This indicates that creation and annihilation fields have the same scalings at bare level, in which case $[\breve{a}(x,t)] = [\tilde{a}(x,t)] = [\breve{p}(x,t)] = [\tilde{p}(x,t)] = d/2$. In particular, two points are worth noting here: one, that $[\breve{a}(x,t)] = [\breve{p}(x,t)]$ is expected as the total density must be conserved; and two, that similar considerations of dimension counting will also be useful at $O(\epsilon)$ for prediction of the hyperuniformity exponent, as will be explained in

Subsection 5.1. The mass term in the passive propagator $-i\omega + \kappa a_0 := -i\omega + \epsilon_p$, determining the distance from criticality, then has dimension $[\epsilon_p] = 2$. The coupling constants also scale according to

$$[\tau_p] = [\alpha_i] = 2 \tag{33}$$

$$[\lambda_i] = [\sigma_i] = 2 - \frac{d}{2} \tag{34}$$

$$[\chi_i] = 2 - d \tag{35}$$

Therefore simply from looking at the scaling dimensions of the coupling constants, it can be concluded that the RO model has an upper critical dimension of $d_c = 4$, above which χ, λ and σ vertices become irrelevant, and our results for the Gaussian approximation hold. Below 4 dimensions, λ and σ vertices become relevant. As noted already (and in Appendix C), if the interactions in (32) were present in the bare action, one would encounter loop corrections with both algebraic (not logarithmic) IR divergences (pointing to a higher $d_c = 6$ instead of 4), and algebraic (not logarithmic) UV divergences.

4.2 Systematic Loop Counting

In $d = 4 - \epsilon$ dimensions, we perform perturbative renormalisation in 1-loop order. Due to the relatively large number of interaction vertices, a careful enumeration of all relevant 1-loop corrections is required. Here we use Euler's theorem for a connected planar graph

$$V - E + L = 1 \tag{36}$$

where V, E, L represent the number of vertices, edges and loops respectively.

Consider loops constructed by the vertices α_i, σ_i and λ_i. We first require the number of additional outgoing legs to match the number of additional incoming legs. We note that an α interaction vertex introduces two extra outgoing legs; a σ interaction vertex introduces two extra outgoing legs and one extra incoming leg; and a λ interaction vertex introduces one extra outgoing leg and two extra incoming legs. From this we obtain (in an obvious notation)

$$2\#\alpha + \#\sigma = \#\lambda \tag{37}$$

After connecting up a selection of these interactions to form a 1-loop correction to some vertex of interest (with initial vertex number V_0 and edge number $E = E_0$) the final vertex number V obeys

$$V = \#\alpha + \#\sigma + \#\lambda + V_0 \tag{38}$$

and the final edge number is

$$E = \#\alpha + \frac{3}{2}\#\sigma + \frac{3}{2}\#\lambda + E_0 \tag{39}$$

where the coefficients encode the fact that each new edge connects two vertices and that α vertices involve two edges but σ and λ involve three.

Substituting the expressions above into (36), we find that $\#\sigma + \#\lambda = 2$. Combined with equation (37), this says that each 1-loop correction must either be constructed by one σ and one λ interaction vertex, or two λ and one α vertex. There are tens of these loops, but most of their corrections cancel eventually; we will show those that will contribute below. A full list that includes non-contributing diagrams is given in Appendix F.

4.2.1 $\lambda\sigma$-type Loops:

Topologically, all loops formed by one σ and one λ vertex look like the leftmost diagram below; from now on we use a black dashed line to represent either an active (red straight) or passive (blue wavy) propagator. The black dots represent vertices of σ, λ or α type.
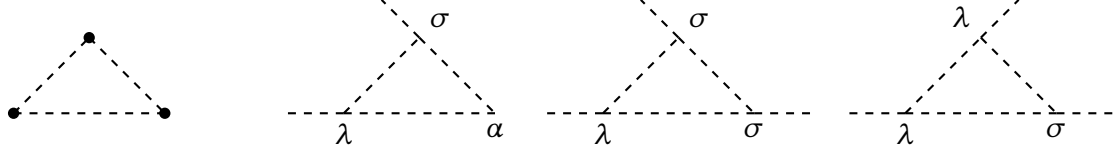
Each node is connected to external legs to form a correction to α, σ and λ vertices, as shown respectively by the remaining three Feynman diagrams. We call these $\lambda\sigma$-type loops because the corresponding loop correction carries a prefactor of $\lambda\sigma$ in the Z-factors in later stages of the RG process. (See Section 4.4 for the standard definition of these Z-factors.) For example in the second diagram an α vertex contribution involves a $(\lambda, \sigma, \alpha)$ triangle, hence the Z-factor for the α-vertex would contain the prefactor $\lambda\sigma\alpha/\alpha = \lambda\sigma$.

When substituting in the active/passive propagators for the black dashed lines, notice that some choices are algebraically (not logarithmically) divergent in $d = 4$. Specifically, these are loop diagrams that include α_3 and $\sigma_{5,6}$, as in (32), which are absent in the bare action but may generically be generated at the RG fixed point. Since we *assume* that the theory is renormalisable overall, as detailed in Section 2.2 (specifically assumptions 2a, 2c there), we implicitly assume that these vertices vanish at the fixed point. In consequence, the set of diagrams generating these vertices at the fixed point must cancel. Therefore all loop contributions at 1-loop order are those constructed without the couplings (32). These are shown below and named for future references:

 (40)
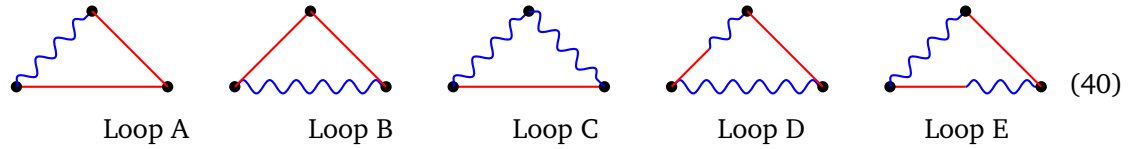
Thereafter, the procedure for calculating the loop corrections contains two steps:
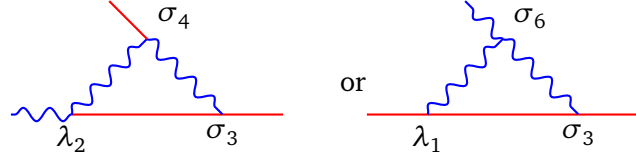
1. Calculate the loop integral for each of these five loops using dimensional regularization.

2. For each interaction vertex, identify the corresponding vertices used for the specific loops.

As an example, we consider Loop C shown in (40) as part of the first step. Using dimensional regularization, the loop integral is evaluated at vanishing external wavenumbers and frequencies,

$$\text{\small(diagram)} \triangleq \int \frac{đ\omega đ q}{(i\omega + \epsilon_p)(i\omega + \epsilon_p)(-i\omega + Dq^2 + \epsilon_a)}$$

$$= \int \frac{d^d q}{(2\pi)^d} \frac{1}{(Dq^2 + \epsilon_p + \epsilon_a)^2} = \frac{(\epsilon_p)^{d/2-2}}{D^{d/2}} \frac{\Gamma(2 - \frac{d}{2})}{2^d \pi^{d/2}} \quad (41)$$

Here, $\epsilon_{p,a}$ are the mass terms for passive and active propagator respectively, with bare values $\epsilon_p = \kappa a_0$ and $\epsilon_a = 0$. We will give their Z-factors, indicating how they are renormalised, in Section 4.4; in particular, we will show $Z_{\epsilon_a} = 1$, i.e. ϵ_a does not flow and stay at its bare

value zero (hence we drop it in the final expression above). In the second step, say we are considering the correction to the σ_3 vertex, or . There are, *a priori* two ways to attach this:
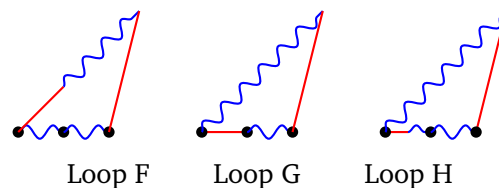

$$\tag{42}$$

However, the σ_6 vertex is eliminated by virtue of our renormalisability assumption (2a in Section 2.2). Therefore, in this example the contribution of the third loop in (40) to σ_3 has a prefactor of $\lambda_2 \sigma_3 \sigma_4$ with symmetry factor 1 coming from the first diagram above. The resulting contribution is $\lambda_2 \sigma_3 \sigma_4 \frac{(\epsilon_p)^{d/2-2}}{D^{d/2}} \frac{\Gamma(2-\frac{d}{2})}{2^d \pi^{d/2}}$. The exact same procedure is done for each of the five loops in (40), and for each interaction vertex α, λ and σ. In Section 4.4, we will show a full list of the resulting corrections after a further discussion of symmetries and effective coupling constants.

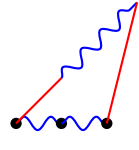### 4.2.2 $\lambda\lambda\alpha$-type Loops:

We turn now to loops constructed by two λ vertices and one α vertex. We first show topological diagrams for these loops and the attachment of external legs for correcting σ and λ vertices:
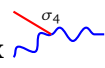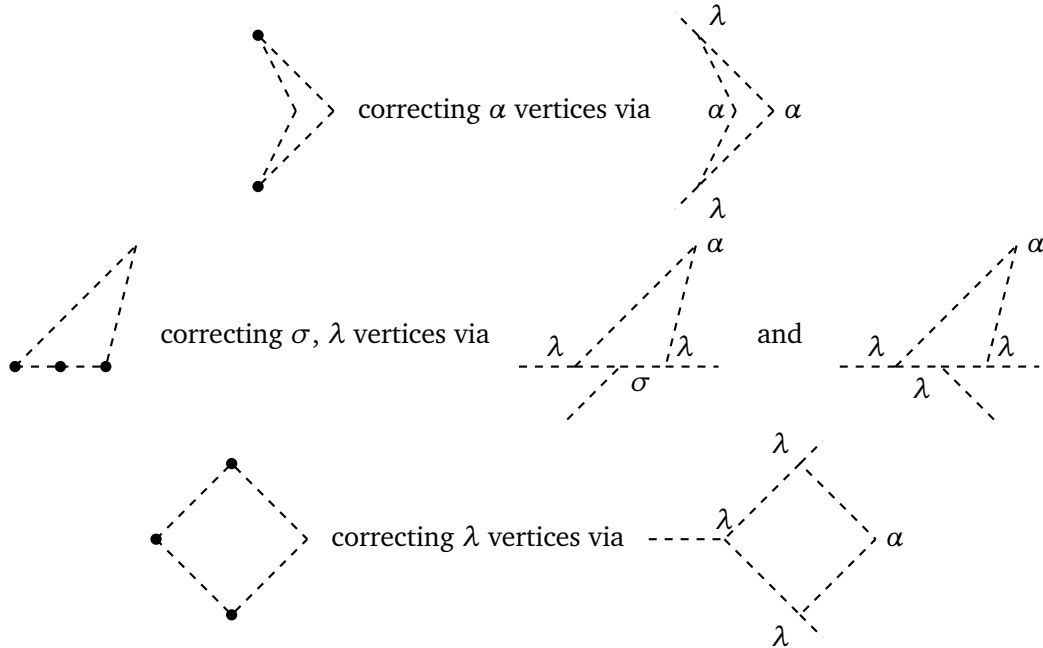

One can check that indeed each loop correction is topologically of the type $\lambda\lambda\alpha$. We find that there are only the three loops of 1-loop order that do not cancel with other loops (compared to the five in (40)) as follows:
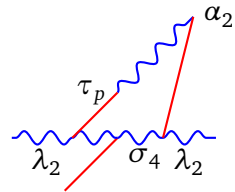

$$\tag{43}$$

Loop F   Loop G   Loop H

Again as an example, we apply dimensional regularization to Loop F:

$$
\triangleq \tau_p \int \dq\, q \left[\frac{1}{2Dq^2(Dq^2+\epsilon_p)^2(\epsilon_p-Dq^2)} \right.
$$
$$
\left. + \frac{1}{4(\epsilon_p)^2(Dq^2+\epsilon_p)(Dq^2-\epsilon_p)} \right] = \frac{1}{4} \frac{\tau_p}{\epsilon_p^2} \frac{(\epsilon_p)^{d/2-2}}{D^{d/2}} \frac{\Gamma(2-d/2)}{2^d \pi^{d/2}} \quad (44)
$$

Then, following the second step described in 4.2.1, we consider how this loop contributes to (say) the σ_4 vertex . We find the exact same scenario as the $\lambda\sigma$-loop example elaborated above: with the prefactor $\lambda_2^2 \alpha_2 \sigma_4$, there is only one way to attach external propagators (hence symmetry factor 1) corresponding to the diagram below:

$$
\triangleq \frac{1}{4} \frac{\lambda_2^2 \alpha_2 \sigma_4 \tau_p}{\epsilon_p^2} \frac{(\epsilon_p)^{d/2-2}}{D^{d/2}} \frac{\Gamma(2-d/2)}{2^d \pi^{d/2}} \quad (45)
$$

Note that there is no contribution from this type of loop in the corrections to either the α vertices (for which it is topologically impossible) or the σ_1, σ_3 vertices (where the leading order correction is 2-loop in general). Note also that in (45), the ϵ_p^2 in the denominator does not induce higher order IR divergences despite going to zero close to the critical point. This is because in the numerator, both τ_p and α_2 also have engineering dimensions $[\tau_p] = [\alpha_2] = [\epsilon_p] = 2$ (in contrast to being marginal). Therefore, at leading order, the prefactor in (45) remains nonsingular.

4.3   Identifying the Effective Coupling Constants

At bare level, there are ten nonlinear interaction vertices (see (31)) and ten interaction coupling constants, together with transmutation τ_p, in the Doi-Peliti action (29). However, many of these arise from shifts in the creation and annihilation fields and they are further locked together because they originate from equal and opposite gain and loss terms of a master equation. In particular, all particle reactions modelled by the master equation conserve the total particle number. (There is no extinction, coagulation, n-tuple annihilation, or branching in the RO system.) The resulting relations (or 'symmetries') must be preserved under RG flow, thus reducing the number of independently relevant couplings. Moreover, any new couplings that are not in (29) but generated at the fixed point must obey these symmetries as well.

There are two ways to derive these field theoretic symmetries: in a bottom-up, nonperturbative, approach we start from the master equation and trace particle number conservation through the various transformations until we reach the coupling constants. In the alternative, perturbative approach, we consider the loop expansions of all couplings and identify which symmetries are maintained in the RG flow. We outline both approaches in the following, starting with the former.

Besides particle number conservation, there is another restriction in the RO class: there are infinitely many absorbing states. This implies that there cannot be a reaction – not even an effective one – in which all reactants are passive particles (the products can be any mix of passive and active particles as long as particle number is conserved).

4.3.1 Proof using Conservation Law:

In the second-quantized version of the master equation, the key observations are that (i) gain and loss terms contain equal numbers of annihilation operators and (ii) that the loss component will always contain an equal number of creation and annihilation operators while the gain will have equal numbers of them if and only if particle numbers are conserved. (For co-agulation, n-tuple annihilation or extinction processes, the gain term contains fewer creation than annihilation operators, whereas for branching processes, the gain term contains more creation than annihilation operators.) Furthermore, if a particle-number-conserving reaction contains a single change in particle type (single active to passive or vice versa), as is the case for our RO action, then loss and gain terms differ only in one creation operator while other creation operators are the same in both terms. This implies that the action must only contain terms that together have the factor $p^\dagger - a^\dagger = \widetilde{p} - \widetilde{a}$. This requirement remains true in the field theory where such operators are (essentially) replaced by their corresponding fields.

The factor $\widetilde{p} - \widetilde{a}$ is present in the bare action (29). In the RG flow, new couplings that emerge must still obey this symmetry: in combination with other such couplings they must maintain the factor $\widetilde{p} - \widetilde{a}$ across all the interaction terms. The couplings that group together in this way attach to vertices that have identical annihilation field legs (in both number and types) and also the same number, but not necessarily same type, of Doi-shifted creation field legs. This requirement implies that

$$\lambda_1 = -\lambda_2 \tag{46a}$$

$$\epsilon_p = \tau_p \tag{46b}$$

$$\epsilon_a = \tau_a (= 0) \tag{46c}$$

$$\alpha_1 = -(\alpha_2 + \alpha_3) \tag{46d}$$
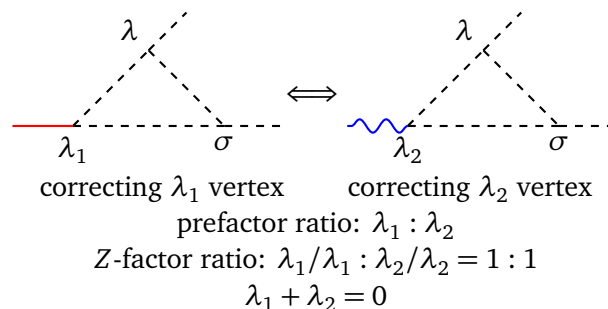
$$\sigma_1 = -(\sigma_3 + \sigma_5) \tag{46e}$$

$$\sigma_2 = -(\sigma_4 + \sigma_6) \tag{46f}$$

$$\chi_1 = -(\chi_2 + \chi_3) \tag{46g}$$

4.3.2 Diagrammatical Proof by Comparing Loop Corrections:

The above line of argument uses a microscopic conservation law on total particle number to constrain the nonlinearities to all orders. However, the results (46) can alternatively be found entirely at field-theoretic level by analyzing the loop expansions of the couplings.

We start with the more straightforward case: establishing the first two symmetries in (46). Here, there is only one outgoing external leg, allowing easy comparison of the loop corrections. There is a *one-to-one correspondence* of loops, with prefactor ratios that cannot change. This means that once we calculate the Z-factors (defined by dividing the loop correction by the corresponding vertex, see Section 4.4), these are exactly the same for each of the first two pairs in (46). A diagrammatic illustration is shown below for $\lambda\sigma$-type loops correcting λ vertices.

correcting λ_1 vertex   correcting λ_2 vertex

prefactor ratio: $\lambda_1 : \lambda_2$

Z-factor ratio: $\lambda_1/\lambda_1 : \lambda_2/\lambda_2 = 1 : 1$

$$\lambda_1 + \lambda_2 = 0$$

Establishing the other symmetries in (46) is slightly less straightforward. Starting with $\lambda\sigma$-type loops, we find that for Loops A, C, D, E (40), the corresponding Z-factor contribution is identical. Take Loop C as an example,

correcting α_1 vertex   correcting α_2 vertex

No contribution of this loop to α_3
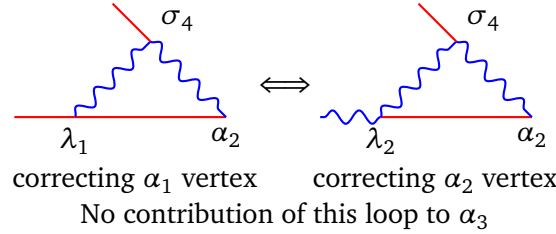
Since $\lambda_1 = -\lambda_2$, and the symmetry factor for both Feynman diagrams is one, the prefactors for the corrections from this loop are equal and opposite. Since at bare level, $\alpha_1 + \alpha_2 = \alpha_3 = 0$ and α_3 is not corrected by this loop, the symmetry $\alpha_1 + \alpha_2 + \alpha_3 = 0$ is preserved.

Subtlety arises however for loops that do also correct α_3 at 1-loop order. For $\lambda\sigma$-type loops, this only happens for Loop B in (40). Diagrammatically,

$$(47)$$

correcting α_1 vertex   correcting α_2 vertex   correcting α_3 vertex
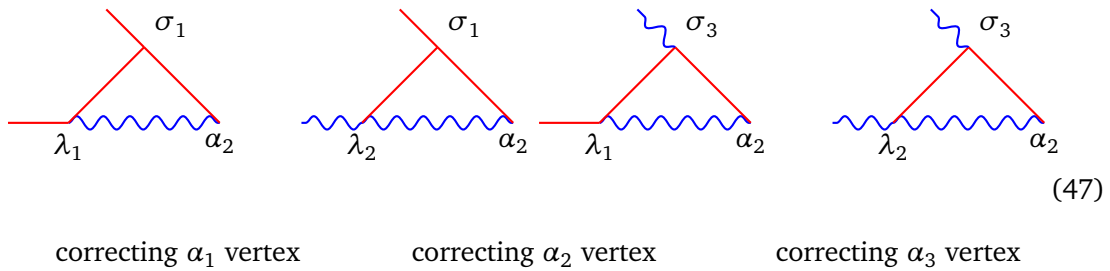
Here the first two Feynman diagrams have a symmetry factor of two (due to the use of σ_1 vertex: the two outgoing legs could interchange), and the other two have a symmetry factor of one. Hence if we consider the correction of this loop to the quantity $(\alpha_1 + \alpha_2 + \alpha_3)$, the contribution from this loop is $(2\lambda_1\sigma_1 + 2\lambda_2\sigma_1 + \lambda_1\sigma_3 + \lambda_2\sigma_3)\alpha_2 \times [\text{loop integral}]$. Therefore, the independently established symmetry $\lambda_1 = -\lambda_2$ ensures that again there are no loop corrections to $\alpha_1 + \alpha_2 + \alpha_3$. It follows that even when a loop corrects also the absent vertices in the action, this does not change the fact that $\alpha_1 + \alpha_2 + \alpha_3 = 0$. A similar check can be done on all three $\lambda\lambda\alpha$-type loops, completing our verification, at 1-loop order, of all the symmetries listed in (46).

4.3.3 Effective Coupling Constants:

As discussed earlier in assumptions 2a, 2c, 2d, vertices (32) cannot be generated at the fixed point, thanks to a cancellation mechanism which we *assume* to be broadly similar to the tricritical Ising model. Nevertheless, we do observe loop corrections to α_3 as we show in (47). These corrections cannot be absorbed into the Z-factors associated with α_3, as α_3 is absent at the RG fixed point; however, ignoring such contributions completely would undermine the basic tenets of the RG, which requires each UV divergence to be taken into account by Z-factors, and violate the symmetry expressed in (47). Thus there has to be a systematic way of absorbing these loop corrections into other Z-factors, ensuring that the contributions to the bare correlators are properly accounted for.

To elaborate this point, we examine how loop corrections to *vertices* contribute to *correlators*. Normally, loop corrections at vertex level are encoded in the corresponding Z-factors, diagrammatically representing the loops with patterned circles:

$$Z_{\alpha_1} = 1 + \quad, \quad Z_{\alpha_2} = 1 + \quad, \quad Z_{\alpha_3} = 1 + \qquad (48)$$

Correlators are calculated by appending external propagators to the vertices. At tree-level, the active-active correlator $\langle \breve{a}\breve{a} \rangle \; \hat{=} \quad \alpha_1 \; + \quad \alpha_2 \; + \quad \alpha_3$, active-passive correlator $\langle \breve{a}\breve{p} \rangle \; \hat{=} \quad \alpha_2 \; + \quad \alpha_3$, and passive-passive correlator $\langle \breve{p}\breve{p} \rangle \; \hat{=} \quad \alpha_3$. Note that transmutation only exists in one direction ($\longrightarrow\!\sim$ is present but not $\sim\!\longrightarrow$).

The tree-level contributions correspond to the '1' in the Z-factors, while loop corrections modify this factor. For example, the active-active correlator is composed of three contributions, each corresponding to Z_{α_1}, Z_{α_2}, and Z_{α_3}. Diagrammatically,

$$\langle \breve{a}\breve{a} \rangle \; \hat{=} \quad + \quad + \quad + \quad + \quad + \qquad (49a)$$

$$\langle \breve{a}\breve{p} \rangle \; \hat{=} \quad + \quad + \quad + \qquad (49b)$$

$$\langle \breve{p}\breve{p} \rangle \; \hat{=} \quad + \qquad (49c)$$

In general, there should be a similarly straightforward correspondence between Z-factors for vertices and corrections to correlators. However, as discussed above, our assumption of renormalisability dictates that α_3, and hence Z_{α_3}, cannot appear at the fixed point. We thus have two options for the Z_{α_3}: either absorb the correction in Z_{α_1} or Z_{α_2}. In the latter case,

$$Z_{\alpha_1} = 1 + \quad, \quad Z_{\alpha_2} = 1 + \quad + \qquad (50)$$

and the correlators obey

$$\langle \breve{a}\breve{a} \rangle \; \hat{=} \quad + \quad + \quad + \quad + \qquad (51a)$$

$$\langle \breve{a}\breve{p} \rangle \; \hat{=} \quad + \quad + \qquad (51b)$$

capturing all loop corrections in (49). In the former case, we instead assign the correction in Z_{α_3} to Z_{α_1}, diagrammatically

$$Z_{\alpha_1} = 1 + \quad + \quad, \quad Z_{\alpha_2} = 1 + \qquad (52)$$

However, in the active-passive correlator, the loop correction $\quad$ is no longer accessible since the vertex α_1 does not enter the correlator associated with $\langle \breve{a}\breve{p} \rangle$. We thus conclude that the systematic way of treating Z_{α_3} is to absorb it into the Z-factor for α_2. We note that this unique choice is a direct result of transmutation working in only one direction.
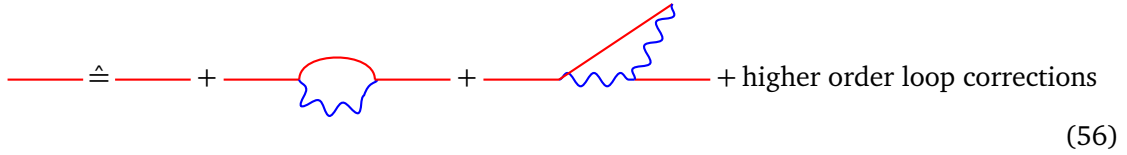
4.4 Beta Functions and Critical Exponents

We now define the various Z-factors (some of which were already discussed) indicating how fields and interaction vertices should be renormalised:

$$D_R = Z_D D \quad \breve{a}_R = Z_{\breve{a}}^{1/2} \breve{a} \quad \tilde{a}_R = Z_{\tilde{a}}^{1/2} \tilde{a} \quad \breve{p}_R = Z_{\breve{p}}^{1/2} \breve{p} \quad \tilde{p}_R = Z_{\tilde{p}}^{1/2} \tilde{p} \tag{53}$$

$$\alpha_R = Z_\alpha \alpha \zeta^{-2} \quad \lambda_R = A_d^{1/2} Z_\lambda \lambda \zeta^{(d-4)/2} \quad \sigma_R = A_d^{1/2} Z_\sigma \sigma \zeta^{(d-4)/2} \tag{54}$$

$$\text{with } A_d := \frac{\Gamma(3-d/2)}{2^{d-1}\pi^{d/2}} \quad \text{(a constant arising from angular integrals)} \tag{55}$$

Here, Γ represents the Gamma function. (Elsewhere in this paper where Γ denotes a vertex functions instead, it is written with subscripts indicating the corresponding vertex or propagator.) Addressing first the field renormalisations, observe that the active propagator is corrected by the following loop diagrams:
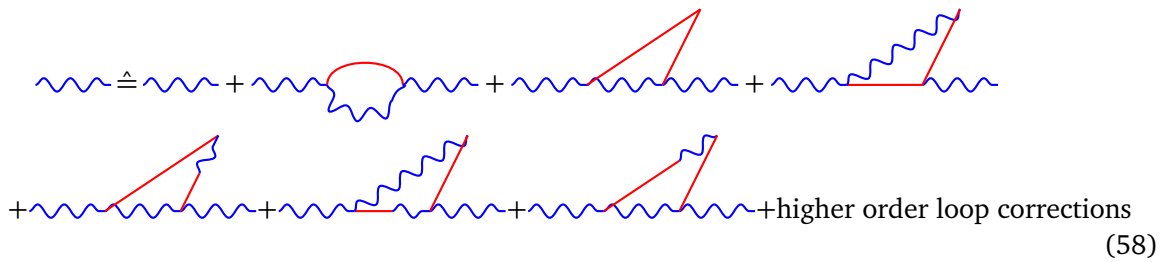

$$\tag{56}$$

This corresponds to the corrections to vertex functions

$$\Gamma_{\text{active propagator}}(q,\omega) = i\omega + Dq^2 + \epsilon_a + \lambda_1 \sigma_3 \int_k \frac{1}{Dk^2 + \epsilon_a + \epsilon_p + i\omega}$$
$$+ \lambda_1 \lambda_2 \alpha_2 \int_k \frac{1}{(D(q-k)^2 + \epsilon_a + \epsilon_p)(D(q-k)^2 + \epsilon_a + \epsilon_p + i\omega)} \tag{57}$$

This vanishes at vanishing wavenumber q and frequency ω. Also, only here we have included ϵ_a as we will use (57) to prove that ϵ_a retain its bare value zero throughout the flow (it is hence dropped in all other loop integrals). Similarly, the passive propagator is corrected by:

$$\tag{58}$$

corresponding to

$$\Gamma_{\text{passive propagator}}(q,\omega) = i\omega + \epsilon_p + \lambda_2 \sigma_4 \int_k \frac{1}{Dk^2 + \epsilon_p + i\omega} + 2\lambda_2^2 \alpha_1 \int_k \frac{1}{(Dk^2 + \epsilon_p + i\omega)(2Dk^2)}$$
$$+ \lambda_1 \lambda_2 \alpha_2 \int_k \frac{1}{(Dk^2 + \epsilon_p)(i\omega + D(q+k)^2 + \epsilon_p)} + \lambda_2^2 \tau_p \alpha_2 \int_k \frac{1}{2Dk^2(Dk^2 + \epsilon_p)(Dk^2 + \epsilon_p + i\omega)}$$
$$+ \lambda_2^2 \tau_p \alpha_2 \int_k \frac{1}{(Dk^2 + \epsilon_p)(i\omega + 2\epsilon_p)(D(q+k)^2 + \epsilon_p + i\omega)}$$
$$+ \lambda_2^2 \tau_p \alpha_2 \int_k \frac{1}{(\epsilon_p - Dk^2)(2Dk^2)(Dk^2 + \epsilon_p + i\omega)} + \frac{1}{(Dk^2 - \epsilon_p)(Dk^2 + \epsilon_p)(i\omega + 2\epsilon_p)} \tag{59}$$

The Z-factors for the fields are evaluated at normalization point $q = \omega = 0$, $\epsilon_p = \zeta^2$ to lowest order in nonlinearities. We use

$$\int \frac{d^d k}{(2\pi)^d} \frac{1}{(\epsilon_p + k^2)^s} = \frac{\Gamma(s - d/2)}{2^d \pi^{d/2} \Gamma(s)} \epsilon_p^{-s+d/2} \tag{60}$$

and apply this to the derivatives $\partial \Gamma_{\text{propagators}} / \partial(i\omega)$. For the active propagator field renormalisation,

$$\begin{aligned}
Z_{\breve{a}}^{1/2} Z_{\tilde{a}}^{1/2} &= \left. \frac{\partial \Gamma_{\text{active propagator}}(q, \omega)}{\partial i\omega} \right|_{(q,\omega)=(0,0)} \\
&= 1 - \lambda_1 \sigma_3 \int_k \frac{1}{(Dk^2 + \epsilon_p)^2} - \lambda_1 \lambda_2 \alpha_2 \int_k \frac{1}{(Dk^2 + \epsilon_p)^3} \\
&= 1 - \frac{\lambda_1 \sigma_3}{D^{d/2}} \frac{A_d \zeta^{-\epsilon}}{\epsilon} - \frac{\lambda_1 \lambda_2 \alpha_2}{\epsilon_p} \cdot \text{finite integral} = 1 - \frac{\lambda_1 \sigma_3}{D^{d/2}} \frac{A_d \zeta^{-\epsilon}}{\epsilon}
\end{aligned} \tag{61}$$

Note the last term is UV-finite and hence dropped from the Z-factor. This is known as minimal subtraction. It also does *not* induce higher order IR divergences being absorbed by the α-term in the numerator (as was shown in (45)). A similar calculation can be done for the passive propagator to obtain

$$Z_{\breve{p}}^{1/2} Z_{\tilde{p}}^{1/2} = \frac{\partial \Gamma_{\text{passive propagator}}(q, \omega)}{\partial i\omega} = 1 - \frac{\lambda_2 \sigma_4}{D^{d/2}} \frac{A_d \zeta^{-\epsilon}}{\epsilon} - \frac{1}{2} \frac{\lambda_2^2 \alpha_2 \tau_p}{\epsilon_p^2} \frac{1}{D^{d/2}} \frac{A_d \zeta^{-\epsilon}}{\epsilon}. \tag{62}$$

Then applying similar calculations to the following derivatives gives

$$Z_{\breve{a}}^{1/2} Z_{\tilde{a}}^{1/2} Z_D = \frac{1}{D} \left. \frac{\partial \Gamma_{\text{active propagator}}(q, \omega)}{\partial q^2} \right|_{(q,\omega)=(0,0)} = 1 \tag{63}$$

$$Z_{\breve{a}}^{1/2} Z_{\tilde{a}}^{1/2} Z_{\epsilon_a} = \left. \frac{\partial \Gamma_{\text{active propagator}}(q, \omega)}{\partial \epsilon_a} \right|_{(q,\omega)=(0,0)} = 1 - \frac{\lambda_1 \sigma_3}{D^{d/2}} \frac{A_d \zeta^{-\epsilon}}{\epsilon} \tag{64}$$

$$Z_{\breve{p}}^{1/2} Z_{\tilde{p}}^{1/2} Z_{\epsilon_p} = \left. \frac{\partial \Gamma_{\text{passive propagator}}(q, \omega)}{\partial \epsilon_p} \right|_{(q,\omega)=(0,0)} = 1 - \frac{\lambda_2 \sigma_4}{D^{d/2}} \frac{A_d \zeta^{-\epsilon}}{\epsilon} - \frac{\lambda_2^2 \alpha_2 \tau_p}{\epsilon_p^2} \frac{1}{D^{d/2}} \frac{A_d \zeta^{-\epsilon}}{\epsilon} \tag{65}$$

Hence, we have found the Z-factors for the mass in the active propagator ϵ_a, diffusion constant D and the distance to the critical point ϵ_p,

$$Z_{\epsilon_a} = 1, Z_D = 1 + \frac{\lambda_1 \sigma_3}{D^{d/2}} \frac{A_d \zeta^{-\epsilon}}{\epsilon}, Z_{\epsilon_p} = 1 - \frac{\lambda_2^2 \alpha_2 \tau_p}{2\epsilon_p^2 D^{d/2}} \frac{A_d \zeta^{-\epsilon}}{\epsilon} \tag{66}$$

Note that the Z-factor for the mass in active propagator to be identically 1 implies that it is not renormalised; this confirms we can safely write the active propagator in its bare, massless form as done in several places above. The scalings of D and ϵ_p give rise to the dynamic exponent z and correlation length exponent $\nu_\perp$ respectively.

As observed from the Z-factors, there are three renormalised dimensionless effective cou-

plings, namely

$$u_R = \frac{\lambda_1 \sigma_3}{D^{d/2}} A_d \zeta^{-\epsilon} \frac{Z_{\lambda_1} Z_{\sigma_3}}{Z_D^{d/2}} \tag{67}$$

$$v_R = \frac{\lambda_2 \sigma_4}{D^{d/2}} A_d \zeta^{-\epsilon} \frac{Z_{\lambda_2} Z_{\sigma_4}}{Z_D^{d/2}} \tag{68}$$

$$w_R = \frac{\lambda_2^2 \alpha_2 \tau_p}{\epsilon_p^2 D^{d/2}} A_d \zeta^{-\epsilon} \frac{Z_{\lambda_2}^2 Z_{\alpha_2}}{Z_{\epsilon_p} Z_D^{d/2}} \tag{69}$$

In the Gaussian theory where all nonlinearities λ's and σ's are suppressed, the renormalised effective couplings u_R, v_R, w_R vanish. Below the upper critical dimension $d_c = 4$, they acquire non-zero values. Importantly, we have defined *combinations* of nonlinearities as effective couplings, because it is only these combinations, not individual nonlinearities, that construct loops and enter beta functions. Such construction of a renormalised effective coupling appears in directed percolation as well [19]. For the $\lambda\sigma$-type loops, there is only one degree of freedom for λ (since $\lambda_1 + \lambda_2 = 0$), and two degrees of freedom for σ (since $\sigma_1 + \sigma_3 = 0, \sigma_2 + \sigma_4 = 0$). Hence there are two effective couplings of this loop type, namely u_R and v_R. For $\lambda\lambda\alpha$-type loops, α only has one degree of freedom ($\alpha_1 + \alpha_2 = 0$), implying that there can only be one effective coupling of this loop type, namely w_R.

RG fixed points are found by setting the beta functions (namely, flow functions for *effective coupling constants*) for the couplings in (67)-(69) equal to zero. As promised in Section 4.2, we present in Appendix E the full list of one-loop corrections to vertices. As shown there, the final beta functions for the effective coupling constants read

$$\beta_u = \zeta \frac{\partial}{\partial \zeta}\bigg|_0 u_R = u_R(\gamma_{\lambda_1} + \gamma_{\sigma_3} - \frac{d}{2}\gamma_D) = u_R\left[-\epsilon - 3u_R - 3v_R - \frac{1}{2}w_R + \mathcal{O}(\epsilon^2)\right] \tag{70}$$

$$\beta_v = \zeta \frac{\partial}{\partial \zeta}\bigg|_0 v_R = v_R(\gamma_{\lambda_2} + \gamma_{\sigma_4} - \frac{d}{2}\gamma_D) = v_R\left[-\epsilon - 2u_R - 4v_R - \frac{1}{2}w_R + \mathcal{O}(\epsilon^2)\right] \tag{71}$$

$$\beta_w = \zeta \frac{\partial}{\partial \zeta}\bigg|_0 w_R = w_R(2\gamma_{\lambda_2} + \gamma_{\alpha_2} - \gamma_{\epsilon_p} - \frac{d}{2}\gamma_D) = w_R\left[-\epsilon - 4u_R - 5v_R - \frac{3}{2}w_R + \mathcal{O}(\epsilon^2)\right] \tag{72}$$

Notice that there is no need to settle degrees of freedom in field renormalisation at this point, since they always show up in pairs of $(\tilde{a}, \breve{a})$ and $(\tilde{p}, \breve{p})$ in the beta functions of the effective coupling constants. Hence the non-Gaussian RG fixed point for the RO universality class obeys the following linear system of equations

$$3u_R + 3v_R + \frac{1}{2}w_R = -\epsilon \tag{73a}$$

$$2u_R + 4v_R + \frac{1}{2}w_R = -\epsilon \tag{73b}$$

$$4u_R + 5v_R + \frac{3}{2}w_R = -\epsilon \tag{73c}$$

Solving these gives $u_R^* = v_R^* = -2\epsilon/9$ and $w_R^* = 2\epsilon/3$. Substituting these results in (66) produces the scaling dimensions for the diffusion constant $[D] = u_R^* = -\frac{2}{9}\epsilon$ and order parameter $[\epsilon_p] = 2 - 1/2w_R^* = 2 - \frac{1}{3}\epsilon$, and thus the dynamic critical exponent z and correlation length exponent $1/\nu_\perp$:

$$D \sim \epsilon_p^{\nu_\perp(z-2)} \Rightarrow z = 2 - \frac{2}{9}\epsilon \tag{74a}$$

$$\xi \sim \epsilon_p^{-\nu_\perp} \Rightarrow \frac{1}{\nu_\perp} = 2 - \frac{1}{3}\epsilon \tag{74b}$$

These match to order ϵ the results found via the mapping onto the quenched Edwards-Wilkinson model (q-EW) via functional RG [14, 16], in line with our assumption 1b in Section 2.2.

A linear stability analysis reveals that the RO fixed point has two stable directions and one unstable direction in the space of effective couplings (u_R, v_R, w_R). Crucially, one of the attractive directions aligns with the vector (u_R^*, v_R^*, w_R^*), indicating the existence of a RG trajectory of the running couplings that connects the Gaussian fixed point in the UV limit to the RO fixed point in the IR limit which, to $O(\epsilon)$, is a straight line in coupling space. This ensures that the RO fixed point, though not fully attractive, can still be accessed perturbatively by appropriately fine-tuning parameters (or, in effect, enforcing cancellation among the algebraic divergences referred to previously). This again bears a high resemblance to the analysis of the tricritical Ising fixed point [45, 46]. In order to determine their critical properties, certain terms in the action are suppressed. Rather than fully characterising the cancellation mechanism at play, we make use of its presence to remove undesired algebraic (not logarithmic) divergences.

There are two further things to note. Firstly, these results give us the sum of anomalous dimensions of the annihilation and creation of fields $[\tilde{a}(x, t)\breve{a}(x, t)] = d+2\epsilon/9$, $[\tilde{p}(x, t)\breve{p}(x, t)] = d-\epsilon/9$. They do not give the dimensions of $\tilde{a}, \breve{a}, \tilde{p}, \breve{p}$ separately; these will be discussed in the next Section. Secondly, the shifts of the annihilation fields (a_0 and p_0) cannot be expressed as any combination of the effective coupling constants u_R, v_R and w_R. Since all universal behaviour to order $\mathcal{O}(\epsilon)$ should be defined by these RG fixed point values, we deduce that these shifts are nonuniversal. This is not surprising: as previously explained, they describe initialisation of the system in the far past.

5 Hyperuniformity and its Exponent

In this Section, we first use our *assumption* that hyperuniformity emerges at the RO critical point (as opposed to divergent fluctuations: see assumption (3) in Section 2.2 above) to *derive* the hyperuniformity exponent ς to order ϵ. We highlight how, in striking similarity to the Gaussian theory (Section 3.2), hyperuniformity emerges by cancellation of separately diverging fluctuations for the active and passive particle species. Thereafter we discuss the implications and physical interpretation of our result for the exponent ς.

5.1 The Hyperuniformity Exponent ς

To find the remaining exponents β and ς we need the dimensions of each field variable separately. Below we show that only one choice (the same as would arise from assuming rapidity reversal in passive particles near criticality [47]) is consistent with hyperuniformity, with all other choices giving *divergent* rather than zero low-q fluctuations at criticality. It is, of course, not unusual for physical knowledge concerning a critical point to resolve ambiguities in an RG calculation, but intriguing that here the requirement of hyperuniformity itself is sufficient to do so.

To see how this works, let us consider $S(q)$. The structure factor for the total density consists of three parts: the active covariance (8), the passive covariance (13) and the active-passive covariance (15). While the complete form for the structure factor is lengthy, we can make the following observations:

- Terms that involve transmutations, such as $\langle \breve{a}\tilde{p}' \rangle$, vanish in the equal-time limit. (The notation is such that a prime indicates that the field has argument $(-q, t)$, whereas without the prime the argument is (q, t). This is similar to the notation in Section 3.2 but the temporal arguments are taken to be equal.) Physically this is because the insertion of an active/passive density cannot instantaneously affect the density of the other species.

- Observables that involve three field operators such as $\langle \breve{a}\tilde{a}'\tilde{a}'\rangle$ also vanish. This is because diagrams that contribute to these, such as ——————×, though allowed in Doi-Peliti field theory, give contributions that contain prefactors of negative powers of ξ hence giving zero contributions.

- Terms of the form of $\langle \breve{a}\rangle\langle \breve{a}\rangle$ cancel collectively due to conservation of total density across the three correlators: $\langle \breve{a}\rangle\langle \breve{a}\rangle + 2\langle \breve{a}\rangle\langle \breve{p}\rangle + \langle \breve{p}\rangle\langle \breve{p}\rangle = 0$ since $\langle \breve{a}\rangle + \langle \breve{p}\rangle = 0$.

Using these observations, the contributing parts can be gathered to give the structure factor for the total density $\rho = \rho_A + \rho_P$ as:

$$\delta^d(0)S(q) := \langle \rho(q,t)\rho(-q,t)\rangle = a_0\langle \breve{a}\tilde{a}'\rangle + \langle \breve{a}\breve{a}'\rangle + \langle \breve{a}\tilde{p}'\rangle + \langle \breve{p}\breve{a}'\rangle + \langle \breve{p}\tilde{p}'\rangle + p_0\langle \breve{p}\tilde{p}'\rangle \quad (75)$$

Here all the correlators are equal-time, with $q, -q$ arguments suppressed for clarity. Evaluating all right hand side correlators at momenta q and q' produces a factor of $\delta^d(q+q')$, which gives rise to $\delta^d(0)$ in Eq. (75). The first two terms represent the active-active density correlator, the next two the active-passive cross correlations, and the final term the passive-passive density correlator. Our RG approach gives no information on amplitude ratios for these terms, so that any cancellations among them cannot be found by comparing prefactors (in contrast to the Gaussian case in (20)). However, their q dependences at criticality are directly set by the scaling dimensions of the four fields, $\breve{a}, \tilde{a}, \breve{p}, \tilde{p}$, and this will be enough for us.

From the anomalous dimensions reported after (73c) above for $[\breve{a}\tilde{a}], [\breve{p}\tilde{p}]$, we observe that at criticality ($\xi \to \infty$) the first of the six terms in (75) scales as $S_1 \sim a_0 q^{2\epsilon/9}$ and the last as $S_6 \sim p_0 q^{-\epsilon/9}$ (after factoring out the $\delta^d(0)$ divergence). The conservation of total particle density (and thus the symmetries proved in 4.3) implies that active and passive fluctuations must scale alike, *i.e.*, the anomalous dimensions for active and passive annihilation fields must match: $[\breve{a}] = [\breve{p}]$. Hence the terms $S_{2,3,4,5}$ all share the same scaling behaviour. Note that, as mentioned already in Section 3.2, the shift a_0 no longer vanishes at criticality as it does in the Gaussian limit. Moreover (see Section 4.4) a_0 cannot be written as a combination of the u, v, w effective coupling constants, nor of the particle field operators, arising in the action (3) or its shifted counterpart. This means that a_0 cannot acquire an anomalous dimension at the fixed point: it merely acts as a non-universal amplitude. (The same is true of p_0, as can separately be confirmed by requiring the exponent β to match the q-EW result.) Accordingly, for the system to be hyperuniform rather than divergently fluctuating at low q (assumption 3 in Section 2.2), S_6 must be cancelled by some combination of the terms $S_{2,3,4,5}$. This requirement *alone* fixes the anomalous dimensions of the fields as $\eta_{\breve{a}} = \eta_{\breve{p}} = \eta_{\tilde{p}} = -\epsilon/18$ and $\eta_{\tilde{a}} = 5\epsilon/18$: only then can all negative powers of q cancel in (75).

Although the terms involved are now divergent rather than finite at $q \to 0$, this cancellation resembles the one found (albeit via a different order of limits) for the Gaussian model in (20) and Fig. 1. As found there, strongly fluctuating active and passive quantities must cross-correlate such that their sum is hyperuniform. Moreover, since every term $S_{i>1}$ in (75) involve just two fields, each has a pure scaling behavior $\xi^0 q^{-\epsilon/9} F_i(q\xi)$ with $F_i(s)$ regular at large s [19]. Hyperuniformity then requires $\sum_{i=2}^{6} F_i(\infty) = 0$, and whatever remains after this cancellation vanishes at criticality where $\xi \to \infty$. (This reasoning would not hold if the individual S_i were, like S, correlators of sums of fields [48].) Accordingly, given that a_0 is not singular as detailed above, the hyperuniformity exponent governing $S(q)$ at the critical point can be read off from S_1 as $\varsigma = 2\epsilon/9$.

As we have emphasised, the critical regime exhibits hyperuniformity of the total density ρ, but not of the active and passive densities separately. Instead, the correlators for these each diverge as $q^{-\epsilon/9}$, confirming a previously known value of $2 - \epsilon/9$ [14] for the exponent $\eta_\perp$ defined via $S_{AA} \sim= q^{-2+\eta_\perp}$ [2]. The anomalous dimensions determined above also imply $\beta = \nu_\perp(d/2 + \eta_{\breve{a}}) = 1 - \epsilon/9$, again matching the results found via the mapping onto the

quenched Edwards-Wilkinson model (q-EW) via functional RG [14, 16] and aligning with assumption 1b in Section 2.2. Indeed, an alternative way of fixing those dimensions is to impose this value of β, already known from the q-EW mapping [14]; hyperuniformity with $\varsigma = 2\epsilon/9$ then follows. (A third route to this same answer would be to make an *ansatz* of an emergent rapidity reversal symmetry [47].)

5.2 The Physics of Hyperuniformity and the Potentially Dangerous Role of Irrelevant Noise

The near-perfect cancellation of active and passive density fluctuations on approach to criticality is remarkable, since the mean density of active particles itself vanishes at the critical point. One may ask: how can fluctuations among a vanishingly small density of active particles perfectly cancel those of a nonvanishing density of passive particles whose fluctuations are either finite (in $d > 4$, where $S_{PP} = p_0$) or even divergent (in $d < 4$, where $S_{PP} \sim q^{-\epsilon/9}$)?

The Gaussian result for $S(q)$ in (20) is again instructive. Here, the ideal-gas-like structure factor (14) for passive particles, $S_{PP} = p_0$, implies that in a cube of linear extent λ such that the passive particle number has mean $N_P(\lambda) = p_0\lambda^d \gg 1$, its standard deviation obeys $\sigma_P(\lambda)^2 \sim p_0\lambda^d$. To cancel the (Gaussian) fluctuations in passive density requires active particles to have the same standard deviation $\sigma_A(\lambda) = \sigma_P(\lambda)$, but now with a mean of only $N_A(\lambda) = a_0\lambda^d$. This can be done, with near-Gaussian fluctuations and without creating negative ρ_A locally, only if $\sigma_A(\lambda) \lesssim N_A(\lambda)$. This requires $p_0^{1/2}\lambda^{d/2} \lesssim a_0\lambda^d$, where $a_0^{-1} \sim \xi^2$, and hence $\lambda \gtrsim \xi^{4/d}$. (Both lengths are here measured in microscopic units.) Hence near-Gaussian fluctuations of the minority active particles *can* cancel the majority passive fluctuations at scales $\lambda \gtrsim \xi$ (which is where hyperuniformity sets in at Gaussian level, see (20)), but only if $d > 4$. In lower dimensions this is not possible. This gives new insight into C-DP's upper critical dimension, $d_c = 4$.

In $d < 4$, the mean number of active particles in a box of size λ now varies as $N_A(\lambda) \sim \lambda^d\rho_A \sim \lambda^d\xi^{-\beta/\nu_\perp} \sim \lambda^{4-\epsilon}$ whereas the variance must obey $\sigma_A(\lambda)^2 = \sigma_P(\lambda)^2 \sim S_{PP}(\lambda^{-1})\lambda^d$, giving $\sigma_A(\lambda) \sim \lambda^{2-4\epsilon/9}$. (This estimate follows from the usual relation between compressibility and structure factor, now applied to a subsystem of size $q^{-1} = \lambda$.) Requiring $N_A(\lambda) \gtrsim \sigma_A(\lambda)$ as before yields $\lambda^{2-5\epsilon/9} \gtrsim \xi^{2-5\epsilon/9}$ and hence $\lambda \gtrsim \xi$. This marginal outcome can be extended beyond order ϵ by use of the scaling relation $2 - \eta_\perp - d = -2\beta/\nu_\perp$ [2]; the details of this calculation can be found in Appendix G. It confirms that in $d < 4$ significantly non-Gaussian fluctuations of ρ_A are needed to avoid negative values: the standard deviation in active particle number is of the same order as its mean in a correlation-length sized box. Without proving that the argument extends across a cascade of shorter scales, as our RG results say it must, we think this makes 'hyperuniformity by cancellation' less mysterious.

A second striking feature of our central result for the RO fixed point, $\varsigma = 2\epsilon/9$, is that it differs from a previous analytical prediction for the hyperuniformity exponent of the C-DP class that arises from the q-EW mapping [17]. Noting that (as confirmed by our calculations) RO and C-DP share common values of the remaining critical exponents $\beta, \nu_\perp, z$, we ascribe this difference to the fact that the q-EW mapping discards the diffusive noise term in (the nonlinear version of) (27). This is in line with our assumption 1c in Section 2.2.

As already seen in Section 3.3, at Gaussian level if the diffusive noise is suppressed, the entire active phase becomes hyperuniform with $\varsigma = 2$ replacing $\varsigma = 0$. Although analytically proven only in the Gaussian case, hyperuniformity is also found numerically, in the active phase away from the critical region, for several fully nonlinear models with similarly suppressed diffusive noise [26]. We therefore believe the diffusive conservative noise, although often deemed irrelevant in the response-field formalism (where it is treated separately from deterministic diffusion), also alters the correlation function exponent. A term in the action (or

field-theoretic operator) that does both these two things is called *dangerously irrelevant* [23].

A dangerously irrelevant operator typically (a) breaks some symmetry and/or (b) cannot be neglected during the calculation of certain observables. We discuss both scenarios below.

One classic example for the former case (breaking of some symmetry) in equilibrium statistical field theory is the Heisenberg model, where the correlation functions perpendicular to the direction of ordering diverge as q^{-2} without cubic anisotropy v, but remains finite (of order $1/v$) with it [23]. Thus the fact that v scales to zero at the Heisenberg fixed point does not mean that the correlator can be found without it. Only if v is strictly zero from the outset, so that rotational symmetry is never broken, can anisotropy be ignored. A more recent example in non-equilibrium systems is when a RG-irrelevant activity changes the scaling behaviour of the density correlator in a two-dimensional active nematic system on a frictional substrate [49]. In both cases, an operator seemingly irrelevant via dimension counting affects the correlation function behaviour, while breaking a conservation law/symmetry.

Similarly, the diffusive noise in RO breaks the 'mass-moment' **p**-conservation law introduced in Section 3.3, and as shown there alters the hyperuniformity exponent throughout the active phase of the Gaussian theory. The presence or absence of the same conservation law also affects hyperuniformity exponents in phase-separated active fluids [42], which are governed by a low-temperature fixed point. Hence it is to be expected that the critical RO fixed point (non-conserved **p**) likewise differs from the C-DP one (conserved **p**) via the action of the irrelevant diffusive noise if this is indeed dangerous as we have argued. If so, the diffusive noise effectively splits the C-DP/RO/q-EW universality class into two. In one sub-class, the diffusive noise is strictly never present (in contrast to scaled to zero under RG flow), so that **p**-conservation is never broken, and the hyperuniformity exponent is $\varsigma = 0 + \epsilon/3$ [17]. In the second sub-class, describing RO as defined in Section 2.2, assumption 1c, there is no conservation law despite the formal irrelevance of the diffusive noise term, and our more singular hyperuniformity exponent $\varsigma = 0 + 2\epsilon/9$ instead prevails.

The latter case of dangerous irrelevance has a formal description [50], where with respect to a physical observable $Y(g_0, g_1(u))$, the coupling u is defined as 'dangerously irrelevant' if despite u flowing to zero, $Y(g_0, g_1(u \to 0))$ is ill-defined, for instance because g_1 contain inverse powers of the irrelevant coupling u. The ϕ^4 coupling for $d \geq 4$ in the Ginzburg-Landau ϕ^4-theory is an example of this, as the magnetisation observable contains inverse powers of the quartic coupling. In the following paragraphs, we explore a possible formal mechanism of how the conserved noise enters the structure factor observable as a dangerous irrelevant operator.

In the conserved **p** case ([17]), the hyperuniformity exponent is predicted from the mapping between the fields ρ and ρ_A via $\partial_t \rho = D\nabla^2 \rho_A$. Note also that a 'statistical-tilt' symmetry ensures that the scaling dimensions obey $[\rho - \rho_c] = [\delta\rho]$ to all orders [16,51] . The latter result is the basis of a previous presentation of the same scaling argument [52] which demands that the density fluctuations are just enough to make some regions drop below ρ_c and become passive (or, on the passive side of the transition, demands that the fluctuations are almost enough to create active regions). Formally, the equality between the scaling dimensions $[\rho - \rho_c] = [\delta\rho]$ in [17] is equivalent to arguing that the local fluctuation amplitude inside a region of size ξ^d, $\delta\rho_\xi$, is comparable to the (global) distance to the critical point $\delta\rho_\infty := \rho - \rho_c$. Writing the structure factor $S(q)$ in terms of a general scaling function $S(q) = q^\varsigma F(g_0 := q\xi, g_1 := \delta\rho_\xi/\delta\rho_\infty)$, the absence of conserved noise thus reduces the general form to $S(q) = q^\varsigma F(g_0 := q\xi, g_1 = O(1))$.

When conserved noise is present (which flows to zero under RG rather than being strictly absent) in the mapping between ρ and ρ_A, the previous equality between scaling dimensions $[\rho - \rho_c] = [\delta\rho]$ is no longer exact and $\delta\rho_\xi$ need not scale as $\delta\rho_\infty$. Notably, our hyperuniformity exponent $\varsigma = 2\epsilon/9$ indicates that local fluctuations prevail, leading to $g_1 = \delta\rho_\xi/\delta\rho_\infty \to \infty$.

Therefore, our reasoning suggests that the difference between the **p**-conserving hyperuniformity exponent $\varsigma = \epsilon/3$ [17] and our **p**-nonconserving one for RO, $\varsigma = 2\epsilon/9$ might fundamentally arise from the difference in $F(g_0, g_1 = O(1))$ and $F(g_0, g_1 \to \infty)$. [2].

Our hyperuniformity prediction is more singular ($\delta\rho_\xi/\delta\rho_\infty \to \infty$), and hence implies that density fluctuations are infinitely larger at criticality than the above reasoning would suggest. This looks paradoxical because it would mean that in a system that is very nearly critical but actually passive – which develops hyperuniformity up to very large scales before ceasing finally to move – the density is above the activity threshold in many spatial regions, in which case how can it be passive overall? This paradox is however resolved by our finding that hyperuniformity emerges by *cancellation of active and passive densities*. Accordingly, whatever the overall density fluctuations are, those of the passive particles alone are at least as big. Thus a fluctuation in which ρ rises above ρ_c in some region does *not* imply that active particles are actually present there.

Our cancellation argument is most easily understood in the active phase, for which we have shown above that the active density fluctuations are large enough to compensate the non-hyperuniform fluctuations of passive particles. But this should still work when considering the passive phase, because in the critical region this spends an extremely long time reducing the low-q density fluctuations towards hyperuniformity while there are still active particles, whose density then finally itself decays to zero. At least on the active side, it is known from simulations that close to criticality large regions of the system are purely passive, and remain so for long periods until a distant patch of activity diffuses into that region [4, 54]. This is only marginally possible with $\varsigma = \epsilon/3$ (since $\rho - \rho_c \sim \delta\rho$), but easy to explain with our exponent $\varsigma = 2\epsilon/9$ (less hyperuniform than the former).

We believe the above arguments to expose an interesting physical distinction between the kinds of density fluctuations arising with and without **p**-conservation, that merits further study by use of microscopic models. However it is not clear at this stage whether such models can easily generate reliable data to distinguish hyperuniformity exponents at the critical point. In particular, existing simulations of **p**-conserving models, while showing hyperuniformity throughout the active phase, have often been interpreted using the same critical exponent (at the absorbing state transition itself) as their non-conserving counterparts [8, 9, 26]. However this might in part stem from the absence until now of any clear theoretical argument to the contrary.

Finally, in the Table below we compare our hyperuniformity exponent for RO calculated to $O(\epsilon)$, with the result found in C-DP/Manna (where centre-of-mass conservation is sustained) [17], calculated to $O(\epsilon^3)$, and with numerical simulations. Subsequent to [8, 9, 26], a numerical work [55] compared critical exponents for RO and a "biased RO" (BRO) model that observes **p**-conservation. There it was found that in three dimensions, while the two models exhibit identical critical exponent β, their hyperuniformity exponents differ somewhat: $\varsigma_{\mathrm{RO}} = 0.24 \pm 0.02$ and $\varsigma_{\mathrm{BRO}} = 0.26 \pm 0.02$. This numerical discrepancy is suggestive but inconclusive; we look forward to future numerical simulations that further elucidate the exponents involved.

6   Concluding Remarks

The hyperuniformity exponent ς describes a signature feature of the Random Organization (RO) universality class, manifested in the physics of the absorbing state transition for dilute colloids under periodic shearing [3–5], in similar transitions at high density in colloids

---

[2]Such reasoning based on comparison of the exponents (and not the engineering dimensions) is analogous to the Harris criterion that determines whether a quenched disorder is relevant to a fixed point [53]

Dimension	RO/**p**-non-conserving	C-DP/Manna/**p**-conserving
$d = 3$	0.22	0.29 {0.33} [17]
$d = 2$	0.44	0.49 {0.66} [17]
$d = 1$	0.66	0.50 {1.00} [17]
$d = 3$ (Numerical)	0.24 ± 0.02 [55]	0.26 ± 0.02 [55]
$d = 2$ (Numerical)	0.45 ± 0.03 [8, 9]	≈ 0.45 [26, 55]
$d = 1$ (Numerical)	0.425 ± 0.025 [8]	0.50 [17]

Table 1: Hyperuniformity exponent comparison in $d = 3, 2, 1$, found to order ϵ (this work, without **p**-conservation) for RO, and to order ϵ^3 via the q-EW mapping of [17] for C-DP/Manna (with **p**-conservation). In the latter, the one-loop prediction to $O(\epsilon)$ also shown as $\{\cdot\}$. Also included are published numerical results for ς with and without **p**-conservation.

and granular media [56–58], and in other reaction-diffusion processes with many absorbing states [2]. Our calculation of this exponent, $\varsigma = 2\epsilon/9$ to order $\epsilon = 4 - d$, has shed light on many aspects of RO physics, including the following:

(i) A form of hyperuniformity is present even in the Gaussian limit of the theory, which prevails in $d > d_c = 4$. Study of this theory shows in detail how hyperuniformity in RO emerges via near-perfect anticorrelation of active and passive densities that are not separately hyperuniform but have finite (for $d > 4$) or divergent (for $d < 4$) fluctuations.

(ii) The RG calculations that we perform at one-loop (order ϵ) expose a range of technical difficulties that have previously hindered development of the perturbative RG for absorbing state transitions of this type. While we have not overcome all of these difficulties from first principles, they can be gathered into a small number of assumptions (laid out in Section 2.2), such as overall renormalizability; a pattern of cancellations among terms akin to that in the 3D tricritical Ising model; and hyperuniformity rather than divergence of the total density fluctuations.

(iii) According to our calculations, diffusive noise splits the C-DP/RO/q-EW universality class into two subclasses. We have argued that it does so by breaking a conservation law on the centre of mass of the total particle density, and that the RO subclass, in which the conservation law is broken by the diffusive noise (which is then dangerously irrelevant) gives a more singular hyperuniformity exponent than one found via a mapping to q-EW (quenched Edwards-Wilkinson) in which the conservation law is sustained. This has implications for the physics of hyperuniformity which merit further study using microscopic models with and without the conservation law [8, 9, 26].

(iv) Our successful completion (albeit subject to the stated assumptions) of a relatively traditional perturbative RG scheme at one-loop level is itself a surprising achievement, since the treatment of other models within the C-DP/RO/q-EW class have required the use of functional RG [16]. The need for functional methods has been ascribed to the presence of infinitely many relevant operators. We do not encounter these in our Doi-Peliti representation, yet our order ϵ results coincide with the functional RG results for the three exponents $(\beta, \nu_\perp, z)$ that are common to the two subclasses mentioned in (iii) above. (We do not expect the same ς for the reasons stated there.) This suggests that the various mappings between different models and field theories that make up the wider C-DP/RO/q-EW universality class may not be completely understood, and in particular that an infinite number of operators in one case may become a finite number in another, at least for the purposes of one-loop calculations. If so, this suggests Doi-Peliti theory might be more widely useful than currently supposed, potentially as a result of retaining particle entities [28].

Our calculations rely on several technical assumptions. First, we assume that the critical

fixed point for RO universality class can be accessed perturbatively by expanding around the Gaussian fixed point to $O(\epsilon)$, with $\epsilon = 4 - d$. While this assumption is standard in field-theoretic renormalisation group analysis, its validity is far from guaranteed here: locating the RO fixed point requires fine-tuning of parameters to enforce the underlying symmetries and conservation laws characteristic of this universality class. An immediate question is whether this calculation, which effectively probes along the stable direction toward a saddle fixed point, holds to higher orders in perturbative RG, or if functional RG methods are required to capture potential non-perturbative features. It is equally intriguing to ask how an absence of diffusive conserved noise could be treated in the Doi-Peliti framework. At present, it is not clear how this can be done, as the stochastic conserved noise and the deterministic diffusion are both implemented in a single term in the Doi-Peliti action. In either case, overcoming these obstacles could greatly extend existing knowledge of the analytical structure of the RO fixed point.

The second crucial assumption is that the spatial correlations in total density are hyper-uniform at the critical fixed point. This allowed us to derive the hyperuniformity exponent without a rigorous proof of the cancellation of diverging amplitudes. Future work could focus on an analytical justification; this would not only strengthen the theoretical foundation of the work presented in this paper, but may reveal intriguing mechanisms driving the emergence of hyperuniformity as well.

We believe our findings to be significant advances towards a more complete understanding of RO physics, and hope they will drive further numerical and experimental investigations of this important class of problems.

Acknowledgements

A   Field-Theoretic RG

For the past few decades, RG analysis within the Doi-Peliti framework has been instrumental in capturing critical phenomena in directed percolation and a wide range of other non-equilibrium phase transitions. It is important to distinguish that most of these successes are built upon the field-theoretic RG approach [19, 27, 32], which differs conceptually from the Wilsonian RG method [59]. Wilsonian RG implements a high-momentum (ultraviolet) cut-off Λ in calculating divergent loop integrals, and by integrating out short-wavelength modes, effectively traces out a flow in theory space. Field-theoretic RG, however, uses dimensional regularisation and minimal subtraction scheme to deal with divergences in the ultraviolet limit. This implies that, instead of constructing a flow of effective theories by integrating out momentum shells, field-theoretic RG focuses on investigating the behaviour of renormalised couplings infinitesimally close to fixed points. In practice, this involves identifying these fixed points where the couplings stay invariant under scale transformations (or 'zooming out'). As a result, while Wilsonian RG often allows one to start directly from the bare theory without extra considerations, performing field-theoretic RG requires particular care in determining what couplings must be included in the action, usually using topological or symmetry arguments.

At one-loop level, the two RG schemes normally give idential critical exponents [48]. From a purely technical point of view, Wilsonian RG regulates ultraviolet divergences by introducing cutoff scales and hence immediately becomes more difficult to handle once nested integrals appear beyond first order in perturbation theory [27]. A deeper insight is that essentially there exists a trade-off between tracking infinitely many operators (Wilsonian RG) and dealing with infinite cutoffs (field-theoretic RG) [48]. In the former, fixed points can still be located even in a theory with finite cutoff; however, the price to pay is that it requires consistent tracking of the flow of all couplings, including those that are irrelevant. On the other hand, field-theoretic approaches allow one to focus on only a finite number of couplings, typically determined through topological or symmetry considerations, but at the cost of achieving scale invariance only when the formal limit of infinite cutoff is taken. Since the dimensional regularisation scheme used to evaluate these infinite integrals relies on perturbative expansions in the parameter $\epsilon = d - d_c$ (with d_c being the upper critical dimension above which Gaussian theory is valid), field-theoretic RG is intrinsically perturbative.

When studying reaction-diffusion processes in Doi-Peliti formalism, unless strong non-perturbative effects are expected, it is often advantageous to pursue the field-theoretic RG approach rather than the Wilsonian one. First, field-theoretic RG avoids the need to track (finitely or infinitely) many coupling constants, as dimensional regularisation naturally handles infinite cutoffs. This is especially helpful as a single reaction often can map to several Doi-Peliti couplings, rendering interpretations or calculations difficult. Second, Wilsonian RG can sometimes run into apparent algebraic divergences which, while often cancelling, must be explicitly tracked along the flow. On the other hand, by starting directly at the fixed point, field theoretic RG avoids this complication.

B   Fixed-Point Manifold and exploiting Redundant Relevant Variables

In this Appendix, we lay out the details underlying assumption 1d in Section 2.2.

In many dynamical field theories such as the ϕ^4 theory, individual coupling constants in the bare theory are also the effective coupling constants of the renormalised one. This means that the RG fixed points are determined by where these coupling constants are scale-invariant under renormalization. Therefore, one can define an effective 'fixed point action' in which all the dimensionless renormalised coupling constants reach their fixed point values. It is thus best practice to include all possible couplings in the bare theory, so as to ensure that the starting point action is within $\mathcal{O}(\epsilon)$ of the unique effective fixed point action. (In particular, if a coupling is omitted that is not $\mathcal{O}(\epsilon)$ but $\mathcal{O}(1)$ at the fixed point, then even the Gaussian level, $\mathcal{O}(1)$ theory will be incorrect.)

In the RO theory constructed from the Doi-Peliti formalism, however, there is no longer a unique fixed point action, but a *manifold* of fixed point actions (the FPM). This is because each microscopic reaction process, under performing second quantisation and the Doi-shift, is separated into several coupling constants; products, rather than individuals, among these different coupling constants are then used to construct loops when doing the RG scheme (see derivation in Section 3). Importantly, each reaction produces several coupling constants, but only specific combinations of them, which we refer to as *effective couplings*, appear in the loop corrections and thus the RG flow functions. Hence, there arise degeneracies of the conventional 'fixed point action'. These degeneracies define the fixed point manifold. (Note that it is not just a manifold whose elements map onto each other under RG, but a manifold of fixed points, each of which maps onto itself.) As discussed at the Gaussian level in Section 3.2, any of these fixed points is a valid representative of the universality class and will therefore have
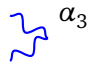
the same critical exponents as any other.

As one decreases the dimension to below four, the Gaussian fixed point manifold is no longer stable. We argue that when we perform the RG for $d = 4 - \epsilon$ dimensions, we first start somewhere on the Gaussian FPM and add a subset of nonlinearities indicated from our microscopic RO theory, which gives an appropriate unstable direction to leave the Gaussian fixed point manifold. Any subset must effectively capture **all** relevant nonlinearities at a certain critical fixed point on the $d = 4 - \epsilon$ fixed point manifold, which we assume to be $\mathcal{O}(\epsilon)$ away from the Gaussian FPM. Our subset of nonlinearities comes from the minimal set of reaction and diffusion processes within the RO universality class that do not promote 'problematic' couplings (as discussed in Appendix C); other potential forms of the fixed point action, while still on the $d = 4 - \epsilon$ FPM, contain these problematic couplings which induce algebraic (not logarithmic) IR/UV divergences. A similar employment of degeneracies caused by redundant parameters is illustrated in [43].

C   Problematic Divergences: Comparison to Tricritical Ising

In the tricritical Ising model, there exist algebraic (not logarithmic) IR divergences $\sim 1/m$ or $\sim \ln m/m$ at the upper critical dimension $d_c = 3$. These problematic diagrams cannot be simply eliminated individually, and are precisely those involving a four-point vertex that is generated under RG even if absent at Gaussian level. However, as one should anticipate, these divergences must cancel collectively in order to give a renormalisable tricritical Ising theory near three dimensions [36], since any remaining quartic term would immediately raise d_c from three to four (and recover the standard Wilson-Fisher critical point, not the tricritical one).

Our RG analysis for RO shows some very similar features to the tricritical Ising model, especially in the IR regime. While we are interested in the RO fixed point which has an upper critical dimension of four, there exist unstable directions to a general theory (such as dynamical percolation [15], or pair contact process [34]) which has an upper critical dimension of six. Also, like in the tricritical Ising, there exist couplings such as , whose inclusion introduces loop integrals that have algebraic divergences in the form of negative powers of m. An example of such a 'problematic' term is as follows:

$$\text{(diagram)} = \frac{1}{\epsilon_p} \int \frac{1}{q^2 + \epsilon_p} d^d q \to \left(\frac{\Lambda^{d-2}}{\epsilon_p} \right) \text{for dimension } d > 2 \qquad \text{(C.1)}$$

	u_4	α_3
Theory	Tricritical in Ising ($d_c = 3$ vs 4)	RO in percolation ($d_c = 4$ vs 6)
Generated?	Yes	Yes
Divergence	$\sim u_4 \cdot 1/m$	$\sim \Lambda^{d-2}/\epsilon_p$
Engineering dimension	$u_4(\zeta) = u_4 \zeta$ (relevant)	Marginal

Table 2: Comparison between four-point vertex in tricritical ising and 'problematic' couplings in RO. Here m, ϵ_p are the mass term for tricritical Ising and RO respectively.

Like the tricritical Ising model, the appearance of algebraic (not logarithmic) IR divergences is likely a result of the RO theory lying in the submanifold of a generic theory with a higher upper critical dimension. However, the additional algebraic UV divergence observed in RO indicates a more serious challenge that we have not so far been able to resolve from

first principles. Therefore, in Section 2, we have phrased this comparison as an **assumption** (2c) that a similar cancellation across super-divergent terms should occur in RO, leading to suppressed $\alpha_3, \sigma_{5,6}$. Evidence for this assumption is that, by making it, we can not only sustain $d_c = 4$ as is known from the q-EW mapping of [13–15], but also reproduce the three standard exponents $\beta, \nu_\perp, z$ of the C-DP/RO/q-EW class found via that mapping [16].

D Effective Couplings at the Gaussian Level

In Section 4.3.3, we argued that to preserve symmetries between coupling constants while suppressing the vertices (32) that induce algebraic (not logarithmic) UV divergences, we consider corrections to α_1 and α_2; the Z-factor for the latter contains corrections to α_3. In this Appendix, we show that this is in accordance with what is observed in the Gaussian structure factors. At Gaussian level, tree-level diagrams for the two-point correlation functions produce

$$\text{Cov}[A(q,t)A(-q,t)] = \alpha_1 \left[\frac{1}{Dq^2 + \tau_p} \right] + a_0 \tag{D.1}$$

$$\text{Cov}[A(q,t)P(-q,t)] + \text{Cov}[A(-q,t)P(q,t)] = -2\alpha_1 \left[\frac{1}{(Dq^2 + \tau_p)} \right] \tag{D.2}$$

$$\text{Cov}[P(q,t)P(-q,t)] = \alpha_3 \left[\frac{1}{\tau_p} \right] + p_0 \tag{D.3}$$

$$\text{Cov}[\rho(q,t)\rho(-q,t)] = a_0 + p_0 - \frac{\alpha_1}{Dq^2 + \tau_p} + \frac{\alpha_3}{\tau_p} \tag{D.4}$$

As stated in assumptions 2a, 2c in Section 2.2, the vertex α_3 needs to be suppressed for a renormalisable theory both for $d > d_c = 4$ and $d < d_c = 4$. Upon suppression of α_3, the two-point correlation functions are solely dependent on $\alpha_1 = -(\alpha_2 + \alpha_3)$. That the theory in $d < 4$ is dependent only on one parameter, namely $\alpha_1 = -\alpha_2$, once α_3 is assumed to vanish, provides some level of confidence for the argument.

E Evaluation of all Loop Corrections

The UV-divergent part of the diagrams required to determine the exponents in this work are listed in Tables 3 and 4 below. These are to be used according to the following guide:

- The first row shows the diagrammatic representations of the loops

- The second row gives the loop integral, calculated using dimensional regularization as shown for example in Eqs. (41) and (45).

- The rows labelled as 'prefactors' (e.g. α_2 prefactors in the third row) provide the couplings whose vertices are placed at the black dots in the loop diagrams of the first row. As an example, for Loop A to correct α_2, the couplings required are $\lambda_2, \sigma_3, \alpha_1$.
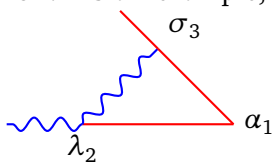
- In the same rows, an underlined 2 is the symmetry factor for Feynman diagrams, which arises if and only if one of σ_1, σ_2 or α_1 appears in the prefactor. This is because σ_1, σ_2

and α_1 have two outgoing active propagators which can be interchanged leading to a symmetry factor of 2.

- The second loop in each table requires caution as highlighted in Section 4.3.3. For simplicity, we have used the prefactors for the symmetric counterparts α_1, σ_1 and σ_2, with an additional negative sign.

- The rows labelled as 'flow function' (e.g. α_2, α_1 flow function in the fourth row) shows what appears in the Z-factor of the corresponding couplings. Each entry in the table is a constant multiple of one of the three effective coupling constants. As an example, the 'u_R' for the first loop in the row of 'α_2, α_1 flow function' is calculated by $\frac{1}{2} \frac{(\epsilon_p)^{d/2-2}}{D^{d/2}} \frac{A_d}{(4-d)} \cdot 2\lambda_2\sigma_3\alpha_1/\alpha_2 = -\lambda_2\sigma_3 \frac{(\epsilon_p)^{d/2-2}}{D^{d/2}} \frac{A_d}{(4-d)} = u_R$.

Loop Integral	$\frac{1}{2}\frac{(\epsilon_p)^{d/2-2}}{D^{d/2}}\frac{A_d}{(4-d)}$	$\frac{(\epsilon_p)^{d/2-2}}{D^{d/2}}\frac{A_d}{(4-d)}$	$\frac{(\epsilon_p)^{d/2-2}}{D^{d/2}}\frac{A_d}{(4-d)}$	$\frac{1}{2}\frac{(\epsilon_p)^{d/2-2}}{D^{d/2}}\frac{A_d}{(4-d)}$	$\frac{1}{2}\frac{(\epsilon_p)^{d/2-2}}{D^{d/2}}\frac{A_d}{(4-d)}$
α_2 prefactors	$2\lambda_2\sigma_3\alpha_1$	$-2\lambda_1\sigma_1\alpha_2$	$\lambda_2\alpha_2\sigma_4$	$\lambda_2\sigma_3\alpha_2$	$\lambda_2\sigma_3\alpha_2$
α_2, α_1 flow function	u_R	$2u_R$	v_R	$-\frac{1}{2}u_R$	$-\frac{1}{2}u_R$
σ_3 prefactors	$2\lambda_2\sigma_3\sigma_1$	$-2\lambda_1\sigma_1\sigma_3$	$\lambda_2\sigma_3\sigma_4$	$\lambda_2\sigma_3\sigma_3$	$\lambda_2\sigma_3\sigma_3$
σ_3, σ_1 flow function	u_R	$2u_R$	v_R	$-\frac{1}{2}u_R$	$-\frac{1}{2}u_R$
σ_4 prefactors	$2\lambda_2\sigma_3\sigma_2$	$-2\lambda_1\sigma_1\sigma_4$	$\lambda_2\sigma_4\sigma_4$	$\lambda_2\sigma_3\sigma_4$	$\lambda_2\sigma_3\sigma_4$
σ_4, σ_2 flow function	u_R	$2u_R$	v_R	$-\frac{1}{2}u_R$	$-\frac{1}{2}u_R$
λ_1 prefactors	$2\lambda_1\lambda_2\sigma_1$	$\lambda_1\lambda_1\sigma_3$	$\lambda_1\lambda_2\sigma_4$	$\lambda_1\lambda_2\sigma_3$	$\lambda_1\lambda_2\sigma_3$
λ_1, λ_2 flow function	u_R	u_R	v_R	$-\frac{1}{2}u_R$	$-\frac{1}{2}u_R$

Table 3: Full list of $\lambda\sigma$-type loops that give non-zero contributions.

Loop Integral	$\frac{1}{4}\frac{(\epsilon_p)^{d/2-2}}{D^{d/2}}\frac{A_d}{(4-d)}$	$\frac{1}{2}\frac{(\epsilon_p)^{d/2-2}}{D^{d/2}}\frac{A_d}{(4-d)}$	$\frac{1}{4}\frac{(\epsilon_p)^{d/2-2}}{D^{d/2}}\frac{A_d}{(4-d)}$
σ_4 prefactor	$\lambda_2^2\alpha_2\sigma_4$	$-2\lambda_1\lambda_2\sigma_2\alpha_2$	$\lambda_2^2\alpha_2\sigma_4$
σ_4, σ_2 flow function	$\frac{1}{4}w_R$	$-w_R$	$\frac{1}{4}w_R$
λ_1 prefactor	$\lambda_1\lambda_2^2\alpha_2$	$\lambda_1^2\lambda_2\alpha_2$	$\lambda_1\lambda_2^2\alpha_2$
λ_1, λ_2 flow function	$\frac{1}{4}w_R$	$-\frac{1}{2}w_R$	$\frac{1}{4}w_R$

Table 4: Full list of $\lambda\lambda\alpha$-type loops that give non-zero or non-cancelling contributions.

Next we provide an example of how to use the tables. We take λ_1 as an example. Reading from the prefactor row of the tables, the vertex function corresponding to λ_1, denoted as Γ_{λ_1}, is corrected as (second to last row in each table):

$$
\begin{aligned}
\Gamma_{\lambda_1} = \lambda_1 &+ 2\lambda_1\lambda_2\sigma_1\frac{1}{2}\frac{(\epsilon_p)^{d/2-2}}{D^{d/2}}\frac{A_d}{4-d} + \lambda_1\lambda_1\sigma_3\frac{(\epsilon_p)^{d/2-2}}{D^{d/2}}\frac{A_d}{4-d} + \lambda_1\lambda_2\sigma_4\frac{(\epsilon_p)^{d/2-2}}{D^{d/2}}\frac{A_d}{4-d} \\
&+ \frac{1}{2}\lambda_1\lambda_2\sigma_3\frac{(\epsilon_p)^{d/2-2}}{D^{d/2}}\frac{A_d}{4-d} + \frac{1}{2}\lambda_1\lambda_2\sigma_3\frac{(\epsilon_p)^{d/2-2}}{D^{d/2}}\frac{A_d}{4-d}
\end{aligned}
\tag{E.1}
$$

The three terms from the second table cancel each other because $\lambda_1 = -\lambda_2$ (note the different factors of $\frac{1}{2}$ and $\frac{1}{4}$ in the 2nd row which shows the loop integrals).

Extracting out the factor λ_1 gives the Z-factor,

$$
\begin{aligned}
Z_{\lambda_1} Z_{\tilde{a}}^{1/2} Z_{\breve{a}}^{1/2} Z_{\breve{p}}^{1/2} &= 1 + \lambda_2 \sigma_1 \frac{(\epsilon_p)^{d/2-2}}{D^{d/2}} \frac{A_d}{4-d} + \lambda_1 \sigma_3 \frac{(\epsilon_p)^{d/2-2}}{D^{d/2}} \frac{A_d}{4-d} + \lambda_2 \sigma_4 \frac{(\epsilon_p)^{d/2-2}}{D^{d/2}} \frac{A_d}{4-d} \\
&\quad + \frac{1}{2} \lambda_2 \sigma_3 \frac{(\epsilon_p)^{d/2-2}}{D^{d/2}} \frac{A_d}{4-d} + \frac{1}{2} \lambda_2 \sigma_3 \frac{(\epsilon_p)^{d/2-2}}{D^{d/2}} \frac{A_d}{4-d} \\
&= 1 + \frac{\lambda_1 \sigma_3}{D^{d/2}} \frac{A_d \zeta^{-\epsilon}}{\epsilon} + \frac{\lambda_2 \sigma_4}{D^{d/2}} \frac{A_d \zeta^{-\epsilon}}{\epsilon}
\end{aligned}
\tag{E.2}
$$

The flow function is hence

$$
\gamma_{\lambda_1} := \zeta \frac{\partial}{\partial \zeta}\Big|_0 \ln Z_{\lambda_1} = -2 + \frac{d}{2} - u_R - v_R - \frac{1}{2}(\gamma_{\tilde{a}} + \gamma_{\breve{a}} + \gamma_{\breve{p}})
\tag{E.3}
$$

Alternatively, the 'flow function' rows of the tables are constructed so that the Z-factors can be read off easily. Each entry is a constant multiple of an effective coupling constant: the constant multiple is calculated by multiplying the loop integral with the symmetry factors, and the effective coupling constant is identified by looking at which interaction vertices are used. Again using λ_1 as an example, its flow function can be read from the tables immediately (last row in each table),

$$
\begin{aligned}
\gamma_{\lambda_1} &= -2 + \frac{d}{2} - \Big(u_R + u_R + v_R - \frac{1}{2}u_R - \frac{1}{2}u_R + \frac{1}{4}w_R - \frac{1}{2}w_R + \frac{1}{4}w_R\Big) - \frac{1}{2}(\gamma_{\tilde{a}} + \gamma_{\breve{a}} + \gamma_{\breve{p}}) \\
&= -2 + \frac{d}{2} - u_R - v_R - \frac{1}{2}(\gamma_{\tilde{a}} + \gamma_{\breve{a}} + \gamma_{\breve{p}})
\end{aligned}
\tag{E.4}
$$

As above for the vertex function, the three terms of the 2nd table cancelled each other.

Similarly, flow functions for other vertices are,

$$
\gamma_{\sigma_3} = -2 + \frac{d}{2} - 2u_R - v_R - \frac{1}{2}(\gamma_{\tilde{a}} + \gamma_{\tilde{p}} + \gamma_{\breve{a}})
\tag{E.5}
$$

$$
\gamma_{\sigma_4} = -2 + \frac{d}{2} - 2u_R - v_R + \frac{w_R}{2} - \frac{1}{2}(\gamma_{\tilde{a}} + \gamma_{\tilde{p}} + \gamma_{\breve{p}})
\tag{E.6}
$$

$$
\gamma_{\alpha_2} = -2 - 2u_R - v_R - \frac{1}{2}(\gamma_{\tilde{a}} + \gamma_{\tilde{p}})
\tag{E.7}
$$

Therefore the renormalisation group beta functions for the effective coupling constants read

$$
\beta_u = \zeta \frac{\partial}{\partial \zeta}\Big|_0 u_R = u_R(\gamma_{\lambda_1} + \gamma_{\sigma_3} - \frac{d}{2}\gamma_D) = u_R\Big[-\epsilon - 3u_R - 3v_R - \frac{1}{2}w_R + \mathcal{O}(\epsilon^2)\Big]
\tag{E.8}
$$

$$
\beta_v = \zeta \frac{\partial}{\partial \zeta}\Big|_0 v_R = v_R(\gamma_{\lambda_2} + \gamma_{\sigma_4} - \frac{d}{2}\gamma_D) = v_R\Big[-\epsilon - 2u_R - 4v_R - \frac{1}{2}w_R + \mathcal{O}(\epsilon^2)\Big]
\tag{E.9}
$$

$$
\beta_w = \zeta \frac{\partial}{\partial \zeta}\Big|_0 w_R = w_R(2\gamma_{\lambda_2} + \gamma_{\alpha_2} - \gamma_{\epsilon_p} - \frac{d}{2}\gamma_D) = w_R\Big[-\epsilon - 4u_R - 5v_R - \frac{3}{2}w_R + \mathcal{O}(\epsilon^2)\Big]
\tag{E.10}
$$

F   List of One-loop Diagrams

Alongside the contributing loops shown in Tables 3 and 4 in Appendix E above, we now show all remaining (non-contributing or cancelling) loops at 1-loop order, for completeness.

(i) The following loops are 'non-contributing', meaning that the loop integral does not show a divergence close to the upper critical dimension, and therefore only gives subdominant corrections.

Non-contributing $\lambda\sigma$-type loops:
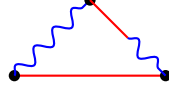
Non-contributing $\lambda\lambda\alpha$-type loops:
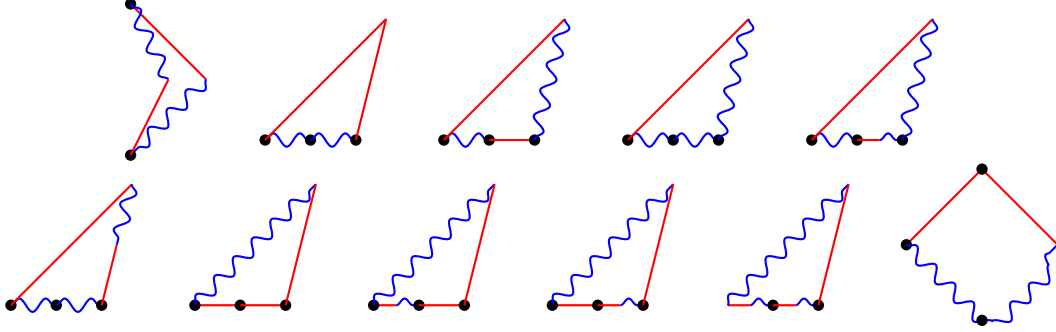
(ii) We now turn to 'cancelling' loops, meaning that although their contribution is of the correct order, they would eventually cancel with each other in vertex corrections. Evaluation of the loop integral gives the same value within each of the pairs shown below, and the prefactors in which these enter any given vertex correction have a ratio of $\lambda_1 : \lambda_2$. By the symmetries (46) established via particle number conservation, $\lambda_1 + \lambda_2 \equiv 0$; as a direct result of this symmetry, the below loop corrections grouped in brackets cancel:
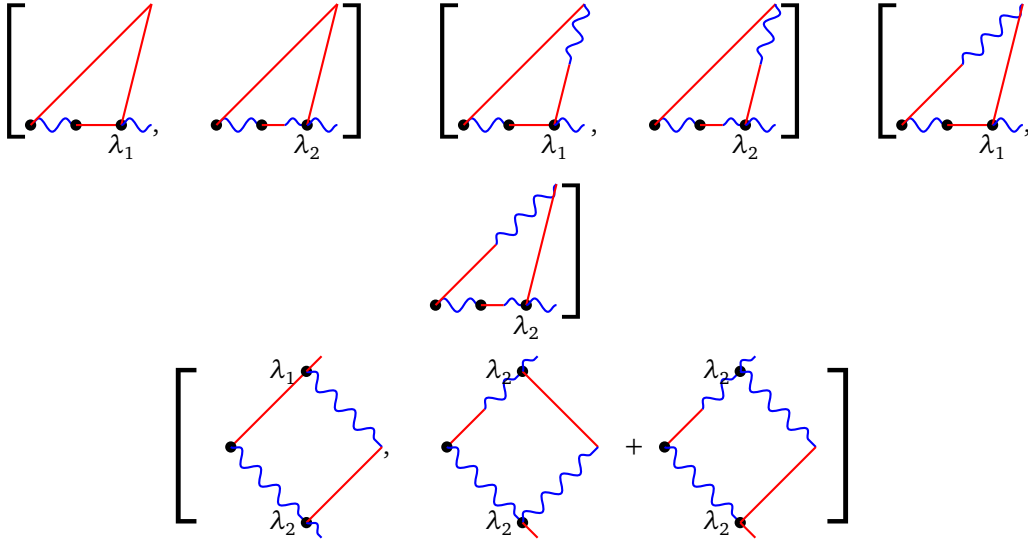
G Cancellation of Density Fluctuations beyond $O(\epsilon)$

In $d < 4$, the mean number of active particles in a box of size λ is given by the active density multiplied by the size of the box, $N_A(\lambda) \sim \lambda^d \rho_A \sim \lambda^d \xi^{-\beta/\nu_\perp}$. For a system of size $\lambda = q^{-1}$, to cancel the finite variance from passive density, the active density variance $\sigma_A(\lambda)^2 = \sigma_P(\lambda)^2 \sim S_{PP}(\lambda^{-1})\lambda^d \sim \lambda^{2-\eta_\perp}$ where $\eta_\perp$ is defined via [2]

$$S_{PP}(q) \sim S_{AA}(q) \sim q^{-2+\eta_\perp}. \tag{G.1}$$

Now to avoid passive densities, we require $N_A(\lambda) \gtrsim \sigma_A(\lambda)$, which gives

$$\lambda^d \xi^{-\beta/\nu_\perp} \gtrsim \lambda^{\frac{2-\eta_\perp+d}{2}} \Rightarrow \lambda^{d+\eta_\perp-2} \gtrsim \xi^{2\beta/\nu_\perp} . \tag{G.2}$$

Using the scaling relation [2]

$$\eta_\perp + d - 2 = 2\beta/\nu_\perp , \tag{G.3}$$

we obtain $\lambda \gtrsim \xi$ to all orders of ϵ.

References

[1] H. Hinrichsen, *Nonequilibrium critical phenomena and phase transitions into absorbing states*, Adv. Phys. **49**, 815 (2000).

[2] S. Lubeck, *Universal scaling behaviour of non-equilibrium phase-transitions*, Int. J. Mod. Phys. B **18**, 3977 (2004).

[3] D. J. Pine, J. P. Gollub, J. F. Brady and A. M. Leshansky, *Chaos and irreversibility in sheared suspensions*, Nature **438**, 997 (2005).

[4] L. Corte, P. M. Chaikin, J. P. Gollub and D. J. Pine, *Random organization in periodically driven systems*, Nat. Phys. **4**, 420 (2008).

[5] L. Corte, S. J. Gerbode, W. Man and D. J. Pine, *Self-organized criticality in sheared suspensions*, Phys. Rev. Lett. **103**, 248301 (2009).

[6] G. I. Menon and S. Ramaswamy, *Universality class of the reversible-irreversible transition in sheared suspensions*, Phys. Rev. E **790**, 061109 (2009).

[7] S. Torquato, *Hyperuniform states of matter*, Phys. Repts. **745**, 1 (2018).

[8] D. Hexner and D. Levine, *Hyperuniformity of critical absorbing states*, Phys. Rev. Lett. **114**, 110602 (2015).

[9] E. Tjhung and L. Berthier, *Hyperuniform density fluctuations and diverging correlations in periodically driven colloidal suspensions*, Phys. Rev. Lett. **114**, 148301 (2015).

[10] S. S. Manna, *Two-state model of self-organized criticality*, J. Phys. A **24**, L363 (1991).

[11] G. Pruessner, *Self-Organised Criticality: Theory, Models and Characterisation*, Cambridge University Press (2012).

[12] G. Willis and G. Pruessner, *Spatio-temporal correlations in the Manna model in one, three and five dimensions*, International Journal of Modern Physics B **32**(05), 1830002 (2018), doi:10.1142/S0217979218300025, https://doi.org/10.1142/S0217979218300025.

[13] G. Pruessner, *Oslo rice pile model is a quenched edwards-wilkinson equation*, Phys. Rev. E **67**, 030301 (2003), doi:10.1103/PhysRevE.67.030301.

[14] P. L. Doussal and K. J. Wiese, *Exact mapping of the stochastic field theory for manna sandpiles to interfaces in random media*, Phys. Rev. Lett. **114**, 110601 (2015).

[15] H. K. Janssen and O. Stenull, *Directed percolation with a conserved field and the depinning transition*, Phys. Rev. E **94**, 042138 (2016).

[16] P. L. Doussal, K. J. Wiese and P. Chauve, *Two-loop functional renormalization group theory of the depinning transition*, Phys. Rev. B **66**, 174201 (2002).

[17] K. Wiese, *Hyperuniformity in the Manna model, conserved directed percolation and depinning*, Phys. Rev. Lett. **133**, 067103 (2024), doi:10.1103/PhysRevLett.133.067103.

[18] X. Ma, J. Pausch and M. E. Cates, *Theory of hyperuniformity at the absorbing state transition*, ArXiv:2310.17391 (2023), 2310.17391.

[19] U. C. Tauber, *Critical Dynamics*, Cambridge University Press, Cambridge (2014).

[20] J. Pausch and G. Pruessner, *Is actin filament and microtubule growth reaction- or diffusion-limited?*, Journal of Statistical Mechanics: Theory and Experiment **2019**(5), 053501 (2019), doi:10.1088/1742-5468/ab081c.

[21] R. Garcia-Millan, J. Pausch, B. Walter and G. Pruessner, *Field-theoretic approach to the universality of branching processes*, Phys. Rev. E **98**, 062107 (2018), doi:10.1103/PhysRevE.98.062107.

[22] K. J. Wiese, *Coherent-state path integral versus coarse-grained effective stochastic equation of motion: From reaction diffusion to stochastic sandpiles*, Phys. Rev. E **93**, 042117 (2016).

[23] P. M. Chaikin and T. C. Lubensky, *Principles of Condensed Matter Physics*, Cambridge University Press (1995).

[24] R. Mari, E. Bertin and C. Nardini, *Absorbing phase transitions in systems with mediated interactions*, Phys. Rev. E **105**, L032602 (2022).

[25] S. Wilken, A. Z. Guo, D. Levine and P. M. Chaikin, *Dynamical approach to the jamming problem*, Phys. Rev. Lett. **131**, 238202 (2023), doi:10.1103/PhysRevLett.131.238202.

[26] D. Hexner and D. Levine, *Noise, diffusion, and hyperuniformity*, Phys. Rev. Lett. **118**, 020601 (2017).

[27] U. C. Täuber, *Renormalization group: Applications in statistical physics*, Nuclear Physics B - Proceedings Supplements **228**, 7–34 (2012), doi:10.1016/j.nuclphysbps.2012.06.002.

[28] M. Bothe, L. Cocconi, Z. Zhen and G. Pruessner, *Particle entity in the doi–peliti and response field formalisms*, Journal of Physics A: Mathematical and Theoretical **56**(17), 175002 (2023), doi:10.1088/1751-8121/acc498.

[29] G. Pruessner and R. Garcia-Millan, *Field theories of active particle systems and their entropy production*, Reports on Progress in Physics **88**(9), 097601 (2025), doi:10.1088/1361-6633/adff30.

[30] D. S. Dean, *Langevin equation for the density of a system of interacting langevin processes*, Journal of Physics A: Mathematical and General **29**(24), L613 (1996), doi:10.1088/0305-4470/29/24/001.

[31] F. Benitez, C. Duclut, H. Chaté, B. Delamotte, I. Dornic and M. A. Muñoz, *Langevin equations for reaction-diffusion processes*, Phys. Rev. Lett. **117**, 100601 (2016), doi:10.1103/PhysRevLett.117.100601.

[32] J. Cardy, G. Falkovich and K. Gawedzki, *Contents*, p. v–viii, London Mathematical Society Lecture Note Series. Cambridge University Press (2008).

[33] H. K. Janssen, *Renormalized field theory of dynamical percolation*, Z. Physik B - Condensed Matter **58**, 311 (1985), doi:10.1007/BF01303673.

[34] F. van Wijland, *Universality class of nonequilibrium phase transitions with infinitely many absorbing states*, Phys. Rev. Lett. **89**, 190602 (2002).

[35] F. J. Wegner, *Some invariance properties of the renormalization group*, Journal of Physics C: Solid State Physics **7**(12), 2098 (1974), doi:10.1088/0022-3719/7/12/004.

[36] A. L. Lewis and F. W. Adams, *Tricritical behavior in two dimensions. ii. universal quantities from the ϵ expansion*, Phys. Rev. B **18**, 5099 (1978), doi:10.1103/PhysRevB.18.5099.

[37] S. Whitelam, L. Berthier and J. P. Garrahan, *Dynamic criticality in glass-forming liquids*, Phys. Rev. Lett. **92**, 185705 (2004), doi:10.1103/PhysRevLett.92.185705.

[38] R. Jack, P. Meyer and P. Sollich, *Mappings between reaction-diffusion and kinetically constrained systems: $A + A \to A$ and the FA model have upper critical dimension $d_c = 2$*, Journal of Statistical Mechanics: Theory and Experiment **2006**, P03006 (2006), doi:10.1088/1742-5468/2006/03/P03006.

[39] A. Lefevre and G. Biroli, *Dynamics of interacting particle systems: stochastic process and field theory*, JSTAT p. P07024 (2007).

[40] J. Cardy and U. C. Täuber, *Theory of branching and annihilating random walks*, Phys. Rev. Lett. **77**, 4780 (1996), doi:10.1103/PhysRevLett.77.4780.

[41] H. Tomita, *Preservation of isotropy at the mesoscopic stage of phase separation processes*, Prog. Theor. Phys. **85**, 47 (1991).

[42] F. D. Luca, X. Ma, C. Nardini and M. E. Cates, *Hyperuniformity in phase ordering: the roles of activity, noise, and non-constant mobility*, Journal of Physics: Condensed Matter **36**(40), 405101 (2024), doi:10.1088/1361-648X/ad5b45, Focus Issue on Hyperuniformity: Exploring Hidden Patterns Across Disciplines.

[43] H. K. Janssen and U. C. Tauber, *The field theory approach to percolation processes*, Annals of Physics **315**, 147 (2005).

[44] H.-K. Janssen, F. van Wijland, O. Deloubrière and U. C. Täuber, *Pair contact process with diffusion: Failure of master equation field theory*, Phys. Rev. E **70**, 056114 (2004), doi:10.1103/PhysRevE.70.056114.

[45] S. Krinsky and D. Furman, *Exact renormalization group exhibiting a tricritical fixed point for a spin-1 ising model in one dimension*, Phys. Rev. Lett. **32**, 731 (1974), doi:10.1103/PhysRevLett.32.731.

[46] B. Nienhuis and M. Nauenberg, *Renormalization-group theory and calculations of tricritical behavior*, Phys. Rev. B **13**, 2021 (1976), doi:10.1103/PhysRevB.13.2021.

[47] F. van Wijland, K. Oerding and H. Hilhorst, *Wilson renormalization of a reaction–diffusion process*, Physica A: Statistical Mechanics and its Applications **251**(1), 179 (1998), doi:https://doi.org/10.1016/S0378-4371(97)00603-1.

[48] D. Amit, *Field theory, the Renormalization Group, and Critical Phenomena*, World Scientific, Singapore, 2nd edn. (1984).

[49] S. Shankar, S. Ramaswamy and M. C. Marchetti, *Low-noise phase of a two-dimensional active nematic system*, Phys. Rev. E **97**, 012707 (2018), doi:10.1103/PhysRevE.97.012707.

[50] M. E. Fisher, *Lecture notes in scaling, universality and renormalization group theory* (1982).

[51] T. Hwa and D. S. Fisher, *Anomalous fluctuations of directed polymers in random media*, Phys. Rev. B **49**, 3136 (1994), doi:10.1103/PhysRevB.49.3136.

[52] R. Dickman and S. D. da Cunha, *Particle-density fluctuations and universality in the conserved stochastic sandpile*, Phys. Rev. E **92**, 020104 (2015), doi:10.1103/PhysRevE.92.020104.

[53] J. M. Luck, *A classification of critical phenomena on quasi-crystals and other aperiodic structures*, Europhysics Letters **24**(5), 359 (1993), doi:10.1209/0295-5075/24/5/007.

[54] C. Reichhardt and C. J. O. Reichhardt, *Random organization and plastic depinning*, Phys. Rev. Lett. **103**, 168301 (2009), doi:10.1103/PhysRevLett.103.168301.

[55] S. Wilken, R. E. Guerra, D. Levine and P. M. Chaikin, *Random close packing as a dynamical phase transition*, Phys. Rev. Lett. **127**, 038002 (2021), doi:10.1103/PhysRevLett.127.038002.

[56] K. H. Nagamanasa, S. Gokhale, A. K. Sood and R. Ganapathy, *Experimental signatures of a nonequilibrium phase transition governing the yielding of a soft glass*, Phys. Rev. E **89**, 062308 (2014).

[57] J. R. Royer and P. M. Chaikin, *Precisely cyclic sand: Self-organization of periodically sheared frictional grains*, Proceedings of the National Academy of Sciences (PNAS) **112**, 49 (2014).

[58] C. Ness and M. E. Cates, *Absorbing-state transitions in granular materials close to jamming*, Phys. Rev. Lett. **124**, 088004 (2020).

[59] K. G. Wilson, *The renormalization group: Critical phenomena and the kondo problem*, Rev. Mod. Phys. **47**, 773 (1975), doi:10.1103/RevModPhys.47.773.